Characterization and Maturation Mechanisms of Succinate Dehydrogenase in Propionate-oxidizing Bacteria

(プロピオン酸酸化細菌におけるコハク酸脱水素酵素の特徴および成熟化機構)

SHIOTA Yusuke

Graduate School of Sciences and Technology for Innovation,
Yamaguchi University

2025 June

CONTENTS

GENERAL INTRODUCTION

Microorganisms live in all kinds of environments, from our bodies to extreme environments on Earth[1,2]. These organisms possess a variety of unique abilities and used these for a variety of applications since[3,4]. The ability of microorganisms is provided by enzymes and know the characteristics of enzymes is important for the utilization of microorganisms.

Some microbial enzymes are species-specific, such as the Polyethylene terephthalate (PET)-degrading enzyme PET hydrolase from *Ideonella sakaiensis*[5], while others are conserved across a wide range of species. One of the universal conserved enzymes is succinate dehydrogenase (SDH), which is conserved in species of all domains, from eukaryotes to archaea and bacteria, catalyzes the oxidation of succinate to fumarate, coupled with quinone reduction[6]. SDH consisting of a flavoprotein subunit, iron sulfur subunit, and a membrane anchor subunit, each of which contains a flavin adenine dinucleotide (FAD) and an iron-sulfur cluster, cytochrome *b* as cofactors[7]. SDH is generally known as an enzyme that is a component of the tricarboxylic acid (TCA) cycle and the membrane electron transfer chain[8] and is central to energy production and metabolism[9]. In addition, SDH is involved in other metabolic pathways, one of which is the propionate oxidation pathway, methylmalonyl-CoA (MMC) pathway[10]. The MMC pathway composed by eleven reactions include three oxidizing reactions, which are energetically unfavorable under the standard condition[11]. These oxidizing reactions are malate oxidation, pyruvate oxidation, and succinate oxidation. Of these, succinate oxidation ($\Delta G^{\circ\prime} = +82$) is the most unfavorable reaction[11]. This most unfavorable reaction catalyzed by SDH is supported by the consumption of metabolic products by syntrophic methanogens and reverse electron transfer[11]. Therefore, SDH is also an important enzyme for microorganisms with the MMC pathway.

One of microorganism with an MMC pathway is *Pelotomaculum thermopropionicum*. *P. thermopropionicum* is one of ten reported species of propionate-degrading bacteria[12], isolated from isolated previously from granular sludge in a thermophilic upflow anaerobic sludge blanket reactor[13]. Previous genomic and transcriptomic analyses have revealed that *Pelotomaculum thermopropionicum* has two types of SDHs: membrane-bound (SDH1) and cytoplasmic (SDH2)[10,14]. SDH from the mesophilic propionate oxidizing bacterium *Syntrophobacter wolinii* requires membrane potential for succinate oxidation[15]. However, there is no report on these in thermophilic propionate oxidizing bacteria. Analysis of SDH from *P. thermopropionicum* would provide functional insights under energetically limiting high-temperature anaerobic conditions. Furthermore, interesting insights into the mechanism of SDH maturation are expected, especially the covalent binding of FAD to the flavoprotein subunit. Covalent binding of flavoprotein subunits to FAD is called flavinylation, and dicarboxylate, heat, and FAD-binding proteins enhance flavinylation[16,17]. However, Gram-positive bacteria very poorly conserved FAD binding proteins[18] and reports on flavinylation are scarce. It is

possible that the universal maturation mechanism of SDH in Gram-positive bacteria can be elucidated by heterologous expression of SDHs from various Gram-positive bacteria, including *P. thermopropionicum*, for which genetic recombination techniques have not been established and the culture complicated, followed by comparative analysis of the heterologously expressed SDHs.

In Chapter 1 of this study, a comparison of the enzymatic activities of the two SDHs in *P. thermopropionicum* cell and investigated the hydrogen production from propionate. In addition, the analysis of the conserved amino acid sequences of the flavoprotein and membrane-bound subunits of SDH in propionate-oxidizing bacteria. In Chapter 2, I attempted to heterologous expression of Gram-positive bacteria SDH and compared SDH activity and maturation of each subunit and examined the maturation mechanism.

CHAPTER 1

Membrane potential-requiring succinate dehydrogenase constitutes the key to propionate oxidation and is unique to syntrophic propionate oxidizing bacteria

ABSTRACT

Propionate oxidation in *Pelotomaculum thermopropionicum* is performed under a thermodynamic limit. The most energetically unfavorable reaction in the propionate oxidation pathway is succinate oxidation. Based on previous genomic and transcriptomic analyses, succinate oxidation in *P. thermopropionicum* under propionate-oxidizing conditions is conducted by the membrane-bound forms of two succinate dehydrogenases (SDHs). We herein examined the activity of SDH, the mechanisms underlying the succinate oxidation reaction in *P. thermopropionicum*, and the importance of the protein sequences of related genes. SDH activity was highly localized to the membrane fraction. An analysis of the soluble fraction revealed that fumarate reductase received electrons from NADH, suggesting the involvement of membrane bound SDH in propionate oxidation. We utilized an uncoupler and inhibitors of adenosine triphosphate (ATP) synthase and membrane-bound SDH to investigate whether the membrane potential of *P. thermopropionicum* supports propionate oxidation alongside hydrogen production. These chemicals inhibited hydrogen production, indicating that membrane-bound SDH requires a membrane potential for succinate oxidation, and this membrane potential is maintained by ATP synthase. In addition, the phylogenetic distribution of the flavin adenine dinucleotide-binding subunit and conserved amino acid sequences of the cytochrome b subunit of SDHs in propionate-oxidizing bacteria suggests that membrane-bound SDHs possess specific conserved amino acid residues that are strongly associated with efficient succinate oxidation in syntrophic propionate-oxidizing bacteria.

1.1 INTRODUCTION

Propionate oxidation, performed by microorganisms in various environments, is energetically unfavorable, particularly in the absence of electron acceptors; the standard Gibbs free energy change is positive for the oxidation reaction[15]. Therefore, propionate oxidation is an unfavorable reaction in methanogenic environments[15,19]. Propionate-oxidizing bacteria reportedly have a syntrophic relationship with hydrogenotrophic methanogens because hydrogen production due to propionate oxidation is facilitated by the consumption of hydrogen by methanogens[19]. Although hydrogenotrophic methanogens enhance propionate metabolism in propionate-oxidizing bacteria, bacteria may perform propionate oxidation close to the thermodynamic equilibrium[20]. These bacteria possess a specific metabolic mechanism related to the oxidation pathways of substrates, particularly propionate.

Two metabolic pathways of propionate oxidation in syntrophic propionate-oxidizing bacteria have been identified: the methylmalonyl coenzyme A (MMC) pathway[10,21] (Fig. 1.1A) and Smithella pathway[22]. The MMC pathway is utilized by most isolated propionate-oxidizing bacteria[19], apart from *Smithella* species[23]. It converts propionate to acetate and carbon dioxide and involves 10 reactions and 3 substrate oxidation steps: malate, pyruvate, and succinate oxidation. Under standard conditions, these oxidation reactions are thermodynamically unfavorable, with succinate oxidation being the most unfavorable[11]. In addition, in the MMC pathway, membrane-associated protein complexes may be solely responsible for succinate oxidation[24]. Using menaquinone as an electron acceptor, membrane-bound succinate dehydrogenase (SDH) catalyzes succinate oxidation in the MMC pathway[11,15,19]. The membrane potential maintained by adenosine triphosphate (ATP) synthase, also known as reverse electron transport, potentially facilitates the SDH-induced reduction of menaquinone. This succinate oxidation-requiring membrane potential has been proposed in *Syntrophobacter wolinii*, a mesophilic propionate-oxidizing bacterium[15]. However, the succinate oxidation reaction has not yet been investigated in thermophilic propionate-oxidizing bacteria. *Pelotomaculum thermopropionicum* SI grows optimally at 55°C[13] and was isolated in a thermophilic upflow anaerobic sludge blanket reactor from granular sludge[25]. A genomic analysis revealed that *P. thermopropionicum* has two types of SDHs[10,26] (Fig. 1.1B). One SDH is membrane bound (SDH1), while the other is cytoplasmic SDH (SDH2), which has not yet been examined in detail. A transcriptome analysis revealed that SDH1 was highly expressed when propionate was used as a substrate and cocultured with a methanogen[14]. Nevertheless, these hypotheses are solely based on genome sequences and transcriptomic data, and the existence of these enzymes has yet to be confirmed. Furthermore, to the best of our knowledge, the relationship between hydrogen production and the membrane potential remains unclear. We herein biochemically analyzed SDH activity in *P. thermopropionicum* cells. We also examined hydrogen production from propionate in a *P. thermopropionicum* monoculture in the presence of several inhibitors. In addition, we performed a sequence homology-based analysis of the catalytic domains of

SDH1 and SDH2 to elucidate the genetic background and phylogenetic differences between proteins and to identify their key amino acid residues.

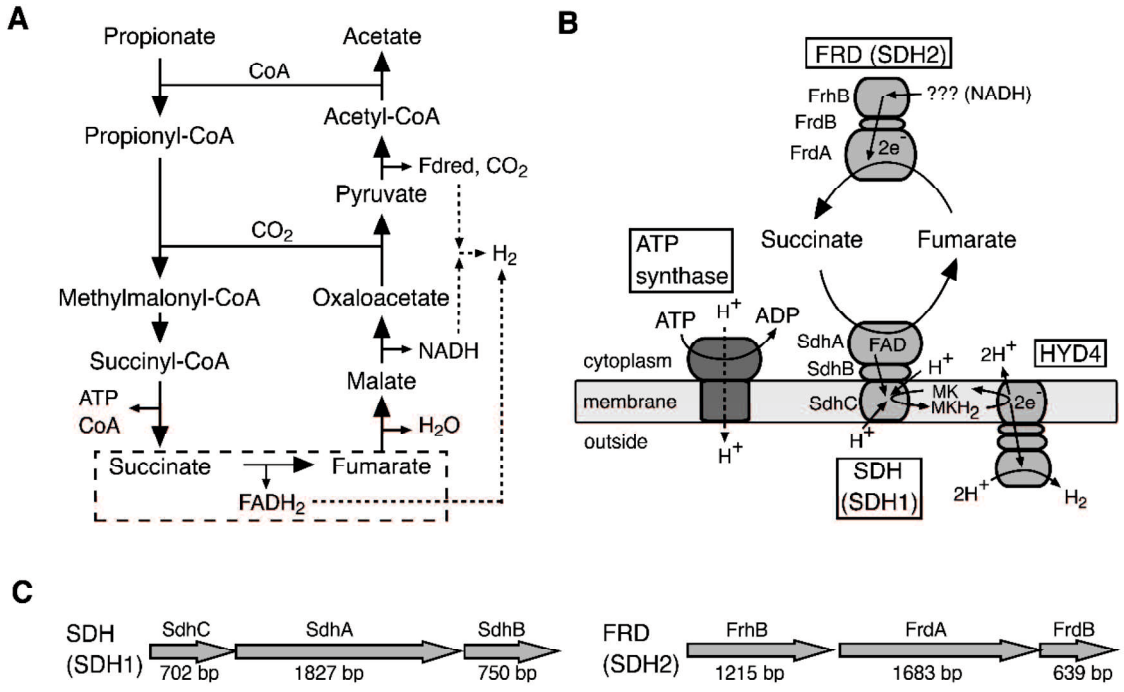

Fig. 1.1 Schematic diagram of succinate oxidation and hydrogen production in the propionate metabolic pathway of *Pelotomaculum thermopropionicum*

(A) The methylmalonyl CoA pathway, a propionate-oxidizing pathway in *P. thermopropionicum*. Modified from previously published papers[10,26]. Details of the membrane-associated reaction enclosed by the dotted line are in panel (B). (B) Schematic diagram of protein complexes involved in succinate oxidation and fumarate reduction and their relationship to the membrane. The number of subunits of ATP synthase is not exact, but the other complexes are with the predicted number of subunits. (C) Cluster structure within the genome of the genes encoding SDH and FRD. Abbreviations: CoA, coenzyme A; NAD, nicotinamide adenine dinucleotide; FAD, flavin adenine dinucleotide; Fdred, reduced ferredoxin; MK, menaquinone

1.2 MATERIALS AND METHODS

1.2.1 Hydrogen production, bacterial strain, and growth and incubation conditions

P. thermopropionicum SI (DSM 13744) was routinely grown on 18 mM fumarate or pyruvate in 50 mL WY medium at 55°C in a 120-mL serum vial with a butyl rubber seal. WY medium containing 0.01% yeast extract in W medium was prepared as previously described[27]. In the enzyme assay, cells were precultured in 50 mL WY medium containing 18 mM fumarate as the substrate. All precultured cells were directly inoculated into 6 L WY medium containing 18 mM fumarate and propionate as substrates in a 10-L medium bottle filled with N_2:CO_2=80:20 gas and sealed with a butyl rubber and plastic cap. The culture was incubated under static conditions at 55°C. Regarding propionate hydrogen production, cells were cultured in 50 mL WY medium containing 18 mM pyruvate as a substrate. The preculture was typically performed for 2 d and then inoculated when growth reached the stationary phase (optical density at 600 nm [OD_{600}] of approximately 0.25–0.3). Regarding the direct inoculation, the preculture (5 mL) was directly inoculated into new media. In the wash inoculation, the preculture was washed as follows: cells were collected from 50 mL of the preculture via centrifugation. Cells were then suspended in 1 mL WY medium after being washed with fresh WY medium three times. One hundred microliters of the cell suspension was inoculated into fresh 50 mL WY medium with 18 mM propionate in a butyl rubber-sealed vial. The vial was incubated at 55°C for ~40 d, and hydrogen was periodically measured in the headspace. When a constant hydrogen production rate was observed, the headspace was substituted with N_2:CO_2=80:20 gas for 3 min in a process known as gas exchange to remove existing hydrogen and reduce oxygen contamination, and the vial was then incubated at 55°C. One hundred microliters of each chemical reagent solution was added via a syringe (Terumo). Carbonyl cyanide m-chlorophenylhydrazone (CCCP), 2-thenoyltrifluoroacetone (TTFA), and N,N-dicyclohexylcarbodiimide (DCCD) were dissolved in pyridine. The additive cofactors were dissolved in water and sterilized by filtration.

1.2.2 Preparation of membrane, soluble, and dialyzed soluble fractions

After an incubation at 55°C for several d when the OD_{600} value was >0.15, cells were collected via centrifugation at 5,000×g at 4°C for 10 min during the stationary phase. The cell pellet was centrifuged again after being washed with saline containing 8.5 mg L–1 NaCl. The pellet was suspended in 10 mL of 10 mM potassium phosphate buffer (KPB, pH 7.0) and subjected to 16,000 psi of pressure in a French press (American Instrument Company). Debris was removed via centrifugation at 8,000×g at 4°C for 15 min, and the supernatant was ultracentrifuged at 100,000×g at 4°C for 60 min using an ultracentrifuge (himac CP80WX, Hitachi). The resulting precipitate was homogenized in 10 mL of 10 mM KPB and used as the membrane fraction. The collected supernatant was dialyzed against 1 L of 10 mM KPB at 4°C every 6 h. The treated solution was used as a soluble fraction.

1.2.3 Enzyme assays

Protein concentrations were measured using the Pierce BCA protein assay kit according to the manufacturer's instructions (Thermo Scientific™). Using a spectrophotometer, routine analyses were conducted at room temperature using 3-mL plastic or 1-mL quartz cuvettes (UV-1850; Shimadzu). Succinate:phenazine methosulfate (PMS)/2,6-dichloroindophenol (DCIP) oxidoreductase activity was measured at 600 nm, 14.52 mM^{-1} cm^{-1} was considered to be the molecular extinction coefficient of DCIP, and one unit of activity corresponded to a reduction of 1 μmol DCIP min^{-1}. The reaction solution contained 16.6 mM KPB, 20 mM succinate, 200 μM PMS, and 100 μM DCIP[28], and the reaction was initiated by the addition of succinate. Succinate:ubiquinone-1 (Q_1) oxidoreductase activity was measured at 275 nm, and we considered 12.25 mM^{-1} cm^{-1} to be the molecular extinction coefficient of Q_1[29]; one unit corresponded to a reduction of 1 μmol Q_1 min–1. The reaction solution contained 45.75 mM KPB, 20 mM succinate, and 50 μM Q_1, and the reaction was initiated by the addition of succinate. NADH:fumarate oxidoreductase activity was measured at 340 nm, and 6.22 mM^{-1} cm^{-1} was considered to be the molecular extinction coefficient of NADH[30]. One unit was equivalent to the oxidation of 1 μmol of NADH min^{-1}. The reaction solution contained 20 mM KPB, 60 mM fumarate, and 5 μM NADH, and the reaction was initiated by the addition of fumarate.

1.2.4 Measurement of the hydrogen content

The gas phase of the cultured vial or bottle was collected using a gas-tight syringe (Hamilton) and applied to a gas chromatography device (GC-8A; Shimadzu) equipped with a thermal conductivity detector (TCD) and a 2×3 mm stainless steel column containing Unibeads C (60/80 mesh) (GL Science). The temperature of the injection port and detector was 150°C, and that of the column was 145°C. The TCD was set to a current of 60 mA, and the flow rate of the carrier gas argon was 30 mL min–1. A calibration curve was produced using standard H2 gas (GL Sciences).

1.2.5 Comparison of sequence data retrieval, phylogenetic tree construction, and gene cluster structures

A total of 1,969 genome sequences were retrieved from the NCBI Reference Sequence (RefSeq) FTP website (ftp.ncbi.nlm. nih.gov/genomes/refseq/). To detect the homologous sequence of SDH/fumarate reductase (FDR), flavoprotein subunit A, we performed a BLASTP search[31] against all of the protein-coding sequences from the 1,969 genomes using the amino acid sequences of three functionally validated protein sequences from *Escherichia coli* BW25113 (SdhA: accession no. AIN31199) and *P. thermopropionicum* SI (Sdh1A: BAF59198 and Sdh2A: BAF59672) as the query. The homologous set was selected by BLASTP based on the criteria of an E-value cut-off of 1e-5 and a minimum aligned sequence length coverage of 70% of a query and hit sequence. All hits from each query were collected, and the merged unique sequence data set was used to build the phylogenetic tree.

The input sequence was aligned using MUSCLE 3.8.31 at the amino acid sequence level and used for phylogenetic construction[32,33]. The MEGAX 10.1.8 package was used to generate a phylogenetic tree to study phylogenetic relationships using the neighbor-joining approach[34,35].

To elucidate the structure of the SDH/FDR gene cluster, 10 genes encoded in the region surrounding each hit were collected. Five of these genes were each encoded in the upstream and downstream regions. Therefore, each hit along with 10 surrounding genes were defined as candidates for the structure of the gene cluster. A homologous group of these candidate proteins was constructed by comparing the all-against-all protein sequences of 1,146 hits and their surrounding proteins using BLASTP[31], followed by Markov clustering with an inflation factor of 1.2[36]. By using an E-value cut-off of 1e-5 and a minimum aligned sequence length coverage of 70% of a query and hit sequence, BLASTP identified the homologous proteins. We investigated flavoprotein subunit A as well as the relationships between the gene cluster structure and phylogenetic location based on the assigned cluster identification of each candidate and their phylogenetic location in SDH/FDR. The domain search was performed using models from the Pfam (https://pfam.xfam.org) and UniProt (https://www.uniprot.org) databases.

1.3 RESULTS

1.3.1 Existence of SDH activity in *P. thermopropionicum* membrane fractions

According to genomic data, *P. thermopropionicum* SI possesses two types of SDHs, designated as SDH1 and SDH2[10] (Fig. 1.1C). SDH1 and SDH2 were located on the membrane and in the cytoplasm, respectively. This was proposed because SDH1 had a transmembrane SdhC subunit, which contained five transmembrane domains, while SDH2 did not have a similar subunit (Table 1.1 and Fig. 1.1B). To confirm the existence of SDHs on the membrane and in the cytoplasm of *P. thermopropionicum*, the enzyme activity of the membrane and soluble fractions of fumarate- and propionate-cultured cells were measured. Cells were harvested upon reaching the stationary phase, indicated by an optical density exceeding 0.15. The cultivation period for these cells ranged from approximately 45 to 55 hours (Fig. 1.2). As cell proliferation progressed, the concentrations of substrates, fumarate and propionate, in the culture supernatant decreased (Fig.1.3). Notably, fumarate was completely consumed, while propionate consumption was gradual. Furthermore, various metabolites produced during propionate metabolism increased with cell growth, though formate production was not observed (Fig. 1.3). Both fractions exhibited succinate:PMS/DCIP oxidoreductase activity; however, it was significantly more active in the membrane fraction than in the soluble fraction (Table 1.2). Furthermore, succinate:Q_1 oxidoreductase activity levels in both fractions were similar to that of succinate:PMS/DCIP oxidoreductase activity (Table 1.2). Since the reduction in Q_1 was considered to be dependent on the cytochrome *b* subunit SdhC of SDH1, which had transmembrane regions (Table 1.1), succinate oxidation in *P. thermopropionicum* was conducted by SDH1 on the membrane. The soluble fraction exhibited higher NADH:fumarate oxidoreductase activity than the membrane fraction (Table 1.2), indicating that the reduction of fumarate occurred in the cytoplasm using NADH as an electron donor.

1.3.2 Conditions of the *P. thermopropionicum* cell preculture for hydrogen production from propionate

Hydrogen production from propionate has been reported in *P. thermopropionicum*[27]. Since the accumulation of hydrogen inhibits the growth of *P. thermopropionicum* during an incubation with propionate, cell growth does not occur when monocultured in propionate; however, when cell activity is present, a very small amount of hydrogen is produced by cells. However, the incubation period required for hydrogen production was markedly longer, ca. 40 d, than that reported in a previous study involving *S. wolinii*, a mesophilic propionate oxidizing bacterium, which produced hydrogen at ca. 5 h. One reason for this difference in the incubation period is the conditions under which *S. wolinii* and other syntrophic, butyrate-oxidizing bacteria were cocultured with methanogens inhibited with bromoethane sulfonate[15,37], whereas *P. thermopropionicum* were monocultured cells[27]. To reduce the time required for propionate hydrogen production, we investigated preculture conditions and culture

additives. Propionate hydrogen production via a direct inoculation was observed when cells were inoculated in a preculture for 2–3 d with pyruvate as a substrate. The partial pressure of hydrogen was slightly reduced for ~10 d, after which it increased to 50 Pa and reached a plateau ~40 d later (Fig. 1.2A). Hydrogen levels did not increase in the absence of propionate (Fig. 1.4A). Similar results were obtained when washed cells were inoculated; however, initial hydrogen production was reduced (Fig. 1.4B). When cells were precultured with fumarate, and even when they were inoculated at a high cell density, an increase in hydrogen was not observed for at least 80 d (data not shown). The difference in the results obtained among preculture substrates may have been due to enzyme expression because the pyruvate and fumarate cultures produced propionate and succinate, respectively, and the operon-like gene cluster coding the enzymes related to the MMC pathway was not highly expressed in the fumarate culture of *P. thermopropionicum*[14]. The timing of the inoculation of the preculture did not affect the time required to increase the level of hydrogen; however, the partial pressure of hydrogen observed immediately following the inoculation had changed (data not shown). Furthermore, the addition of 200 nM cofactors, including cobalamin, pantothenate, thiamine, and biotin, into the media with propionate before the cell incubation did not affect the incubation period needed for an increase in the level of hydrogen (data not shown). Although we did not identify any conditions to shorten the period of hydrogen production, we noted high reproducibility when the preculture was performed using pyruvate as a substrate and cells were incubated for >40 d (Fig. 1.4B). Following gas exchange in the headspace of the vial producing hydrogen from propionate, the partial pressure of hydrogen had finally reached 40–100 Pa (Fig. 1.3).

1.3.3 Effects of an uncoupler and inhibitors on hydrogen production from *P. thermopropionicum* incubated in propionate-containing media

Under propionate-oxidizing conditions, succinate oxidation constituted the first oxidation step in the MMC pathway (Fig. 1.1A). This oxidation reaction generated menaquinol, which is required for hydrogen production, and there were no other predicted enzymes besides SDH that produced menaquinol under propionate-oxidizing conditions (Fig. 1.1B). Furthermore, succinate oxidation was largely responsible for hydrogen production from propionate in *P. thermopropionicum*. Therefore, membrane-bound SDH appeared to be the key enzyme in the MMC pathway. In addition, succinate oxidation in a mesophilic propionate oxidizing bacterium was previously shown to be dependent on the membrane potential maintained by ATP synthase[11,15]. To clarify whether succinate oxidation in *P. thermopropionicum* depended on the membrane potential, we examined the inhibitory effects of the uncoupler CCCP on hydrogen production in *P. thermopropionicum* cells incubated with propionate. The addition of 10 μM CCCP inhibited hydrogen production from propionate, while 100 μM CCCP completely suppressed hydrogen production (Fig. 1.5A). Furthermore, we measured propionate hydrogen production using DCCD, an ATP synthase inhibitor. Propionate hydrogen production was

reduced by 10 μM DCCD and completely inhibited by 100 μM DCCD (Fig. 1.5B). These results indicate that *P. thermopropionicum* requires an ATP synthase-maintained membrane potential for propionate hydrogen production. To clarify the relationship between quinones and propionate hydrogen production, we utilized TTFA, which competitively inhibits quinone-binding sites[38,39]. We observed a decrease in hydrogen production following the addition of >100 μM TTFA (Fig. 1.5C). TTFA also inhibited succinate:Q_1 oxidoreductase activity in the membrane fraction to a small degree (Fig. 1.6). These results suggest that membrane bound SDH1 was essential for succinate oxidation during hydrogen production by *P. thermopropionicum* incubated in propionate-containing media.

1.3.4 Phylogenetic distribution of flavoprotein subunits and importance of the cytochrome *b* subunit of SDH

The importance of membrane-associated SDH in *P. thermopropionicum*, a thermophilic propionate-oxidizing bacterium, has increased interest in conserving the amino acid sequence of SDH subunits in propionate-oxidizing bacteria. SDH comprises three or four subunits, including the flavoprotein subunit, SdhA, the Fe-S cluster subunit, SdhB, and the cytochrome b subunit, SdhC (with SdhD)[40]. To examine the phylogenetic distribution of SDH, we compared homologous flavoprotein subunit protein sequences. In the SdhA and FrdA homolog phylogenetic tree, the flavoprotein subunits SDH and FRD, respectively, indicated that the Sdh1A of *P. thermopropionicum* was contained within clade 7 (Fig. 1.7). Although this phylogenetic analysis was based on protein sequence similarities and did not necessarily provide a phylogenetic classification, clade 7 contained the SdhA of the mesophilic syntrophic propionate-oxidizing bacterium *Syntrophobacter fumaroxidans* (Fig. 1.7). Conserved amino acid sequences were observed among clade 1, containing *E. coli* SdhA, clade 5, containing *E. coli* FrdA, and clade 7. Alignment revealed that FAD-binding motifs (PROSITE:PS00504) were similar and also that the most well-known FAD binding residue His43[41,42] was highly conserved (Fig. 4A). The eighth amino acid was glutamine (Gln) in clades 1 and 7 and glutamic acid (Glu) in clade 5 (Fig. 1.8A). Gln and Glu were consistent with the substrate specificities of succinate:ubiquinone oxidoreductase (SQR) and menaquinol:fumarate oxidoreductase (QFR) as succinate and fumarate, respectively[43]. These results suggest that clade 7 belongs to the SQR type. Furthermore, clades 1 and 5 both had valine at the fifth position, which was unique to *Pelotomaculum* (Fig. 1.8A).

We investigated the relationships between the Fe-S cluster and cytochrome b subunits and the phylogeny of the flavoprotein subunit by summarizing the structures of the cluster of protein homologs comprising SDH/FRD based on the phylogenetic tree of the flavoprotein subunit (Fig. 1.7). Although the Fe-S cluster subunit (cluster 1) was always associated with the flavoprotein subunit (cluster 0, FAD-binding motif), the third and fourth components of each clade were distinct (Fig. 1.7). Cluster 29, which is affiliated with clade 7, contained the SdhC gene of *P. thermopropionicum* and the cytochrome b subunits of *S. fumaroxidans*, *Desulfovibrio gigas*, and *Wolinella succinogenes*. The

alignment and conserved sequences of cluster 29 suggested that the His motif for heme binding (His93, His120, His143, and His182 for *W. succinogenes*) was highly conserved (Fig. 1.9). Additionally, the residues related to the E-pathway for transporting protons outside the membrane into the cytoplasm in the cytochrome b subunit of *W. succinogenes* (His44, Glu180)[40,44] were previously reported to be His38, Glu164, and Glu193 in the cytochrome b subunit of *D. gigas*[42]. These residues were conserved in *P. thermopropionicum* (His41, Glu181, and Glu199) and *S. fumaroxidans* (His37, Glu167, and Glu196) (Fig. 1.9). The E-pathway theoretically reduces the membrane potential of succinate oxidation[40]. These findings suggest that syntrophic propionate-oxidizing bacteria retain the heme-binding and E-pathway motifs. Notably, Asp63 in SdhC of *P. thermopropionicum* was changed from Glu, which is a putative menaquinone-binding site predicted in *D. gigas*[42] (Fig. 1.8B). Furthermore, the residue was conserved in the SdhCs of the obligate syntrophic propionate-oxidizing bacteria *Pelotomaculum propionicicum* and *Pelotomaculum shinckii*[45] (Fig. 1.8B), suggested that this amino acid residue evolved in syntrophic propionate-oxidizing bacteria requiring the membrane potential for succinate oxidation.

Table 1.1 Predicted genes for succinate oxidation and hydrogen production in *P. thermopropionicum*

*TM: transmembrane region numbers from UniProt information. †TAT: +, presence of twin-arginine translocation signal peptide.

Enzyme	Locus_tag	UniProt	Protein	Annotation	Electron transfer	Size (aa)	TM *	TAT †
SDH1 SDH	PTH_1016	A5D3J0	Sdh1C > SdhC	succinate dehydrogenase/fumarate reductase, cytochrome b subunit	Succinate <-> MK	233	5	
	PTH_1017	A5D3J1	Sdh1A > SdhA	succinate dehydrogenase/fumarate reductase, flavoprotein subunit		608	0	
	PTH_1018	A5D3J2	Sdh1B > SdhB	succinate dehydrogenase/fumarate reductase, Fe-S protein subunit		249	0	
SDH2 FRD	PTH_1490	A5D270	Sdh2B > FrdB	succinate dehydrogenase/fumarate reductase, Fe-S protein subunit	Fumarate <->?	212	0	
	PTH_1491	A5D271	Sdh2A > FrdA	succinate dehydrogenase/fumarate reductase, flavoprotein subunit		560	0	
	PTH_1492	A5D272	FrhB	coenzyme F420-reducing hydrogenase, beta subunit		404	0	
HYD1	PTH_0668	A5D4I9		Iron only hydrogenase large subunit, C-terminal domain, containing ferredoxin	? <-> H_2	530	0	+
	PTH_0669	A5D4J0	HybA	Fe-S-cluster-containing hydrogenase components 1		271	0	
	PTH_0670	A5D4J1		Hypothetical protein		89	1	
HYD2	PTH_1377	A5D2H3		hypothetical hydrogenase subunit	NADH, Fd red <-> H_2	624	0	
	PTH_1378	A5D2H4	NuoF	NADH:ubiquinone oxidoreductase, NADH-binding (51 kD) subunit		650	0	
	PTH_1379	A5D2H5	NuoE	NADH:ubiquinone oxidoreductase 24 kD subunit		192	0	
HYD3	PTH_2010	A5D0Q2		hypothetical hydrogenase subunit	NADH, Fd red <-> H_2	574	0	
	PTH_2011	A5D0Q3	NuoF	NADH:ubiquinone oxidoreductase, NADH-binding (51 kD) subunit		551	0	
	PTH_2012	A5D0Q4	NuoE	NADH:ubiquinone oxidoreductase 24 kD subunit		162	0	
HYD4	PTH_1701	A5D1L0	HyaA	Ni,Fe-hydrogenase I small subunit	MK <-> H_2	332	0	+
	PTH_1702	A5D1L1	HyaB	Ni,Fe-hydrogenase I large subunit		482	0	
	PTH_1703	A5D1L2	HybA	Fe-S-cluster-containing hydrogenase components 1		277	0	
	PTH_1704	A5D1L3	NrfD	NrfD participates in the transfer of electrons from quinone pool into the terminal components		389	10	

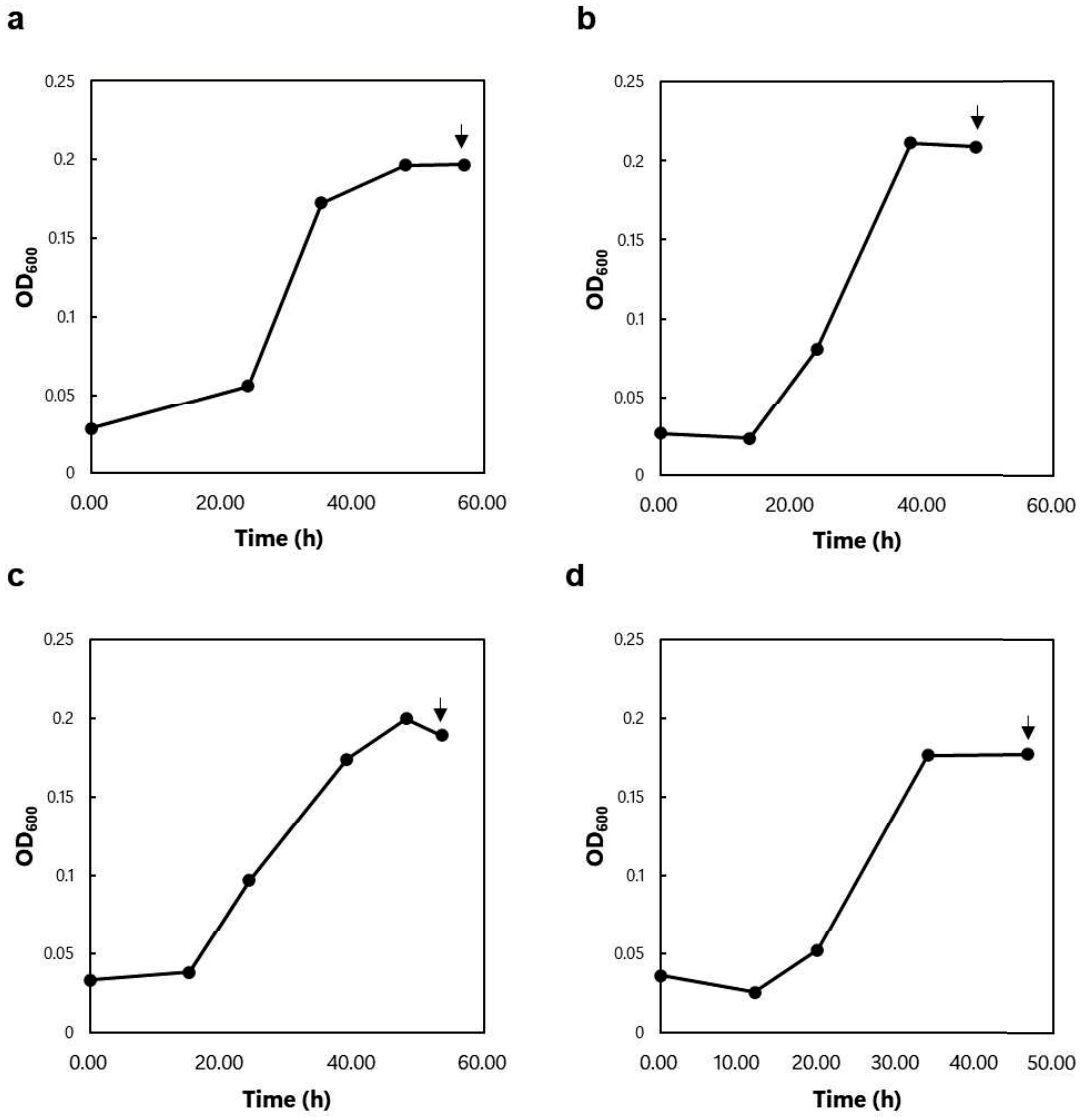

Fig. 1.2 Cell Growth Curves with Fumarate and Propionate as Substrates.

Arrows indicate the timing of cell harvesting. a to d represent the growth of cells used for four independent activity measurements.

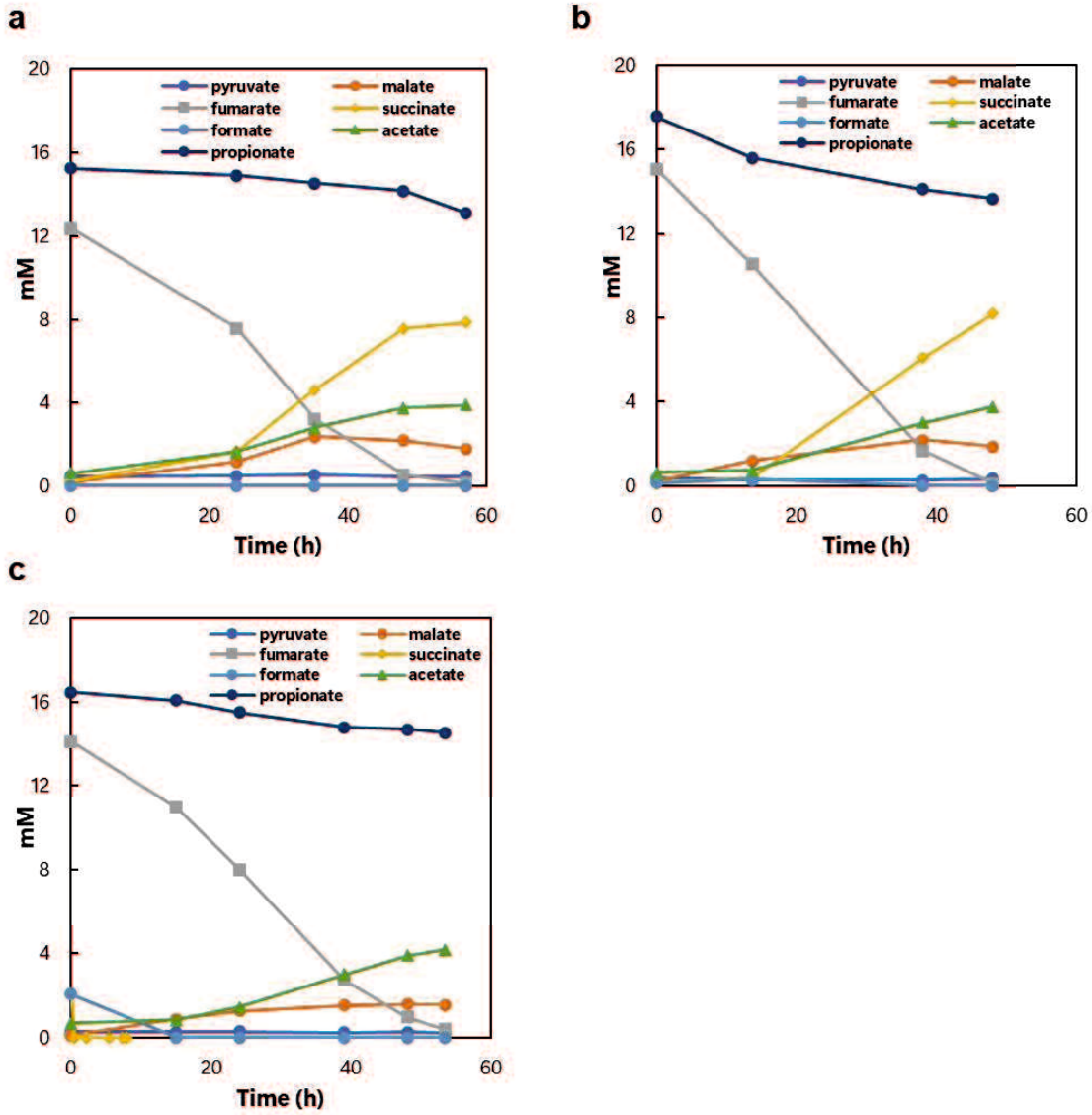

Fig. 1.3 ***P. thermopropionicum*** **metabolite analysis.**

a-c in this analysis represents the metabolites at points a-c in Fig.1. 2. Metabolites were quantified using high-performance liquid chromatography (HPLC). HPLC analyses were performed using an Alliance e2695 (Waters) equipped with a quaternary pump, a standard autosampler, a thermostatic column compartment, RI detector, and UV detector. The mobile phase was 0.1 mM perchloric acid.

Table 1.2 Enzyme activity of membrane and soluble fractions prepared from *P. thermopropionicum* cells

	Membrane fraction*	Soluble fraction*
Succinate:PMS/DCIP oxidoreductase activity (mU/mg)	96.8 ± 68.1	3.7 ± 2.7
Succinate:Q_1 oxidoreductase activity (mU/mg)	43.9 ± 22.3	2.9 ± 3.6
NADH:fumarate oxidoreductase activity (mU/mg)	5.7 ± 5.3	35.7 ± 17.7

*± standard deviations (n = 4)

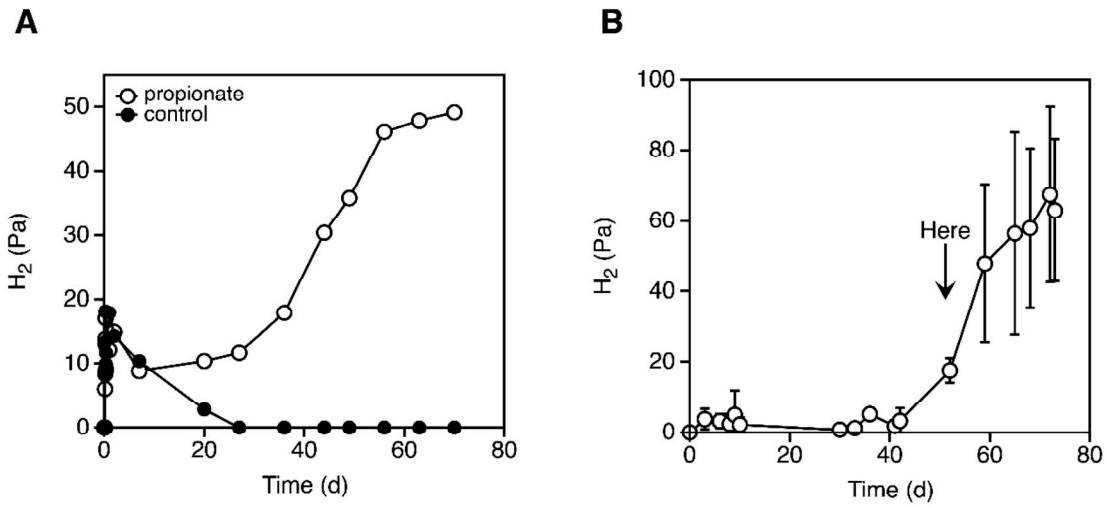

Fig. 1.4 Propionate hydrogen production by *P. thermopropionicum* cells.

Hydrogen in the headspace of vials was detected via gas chromatography. (A) Time course of hydrogen partial pressure in the headspace of vials with media with (open circles) or without (closed circles) propionate-containing media. An aliquot of preculture was directly inoculated with pyruvate grown cells for inoculation. (B) Washing inoculation was used to conduct repeated propionate incubations. The error bars represent the standard deviations for each of the three samples. The arrow indicates the typical timing of gas exchange.

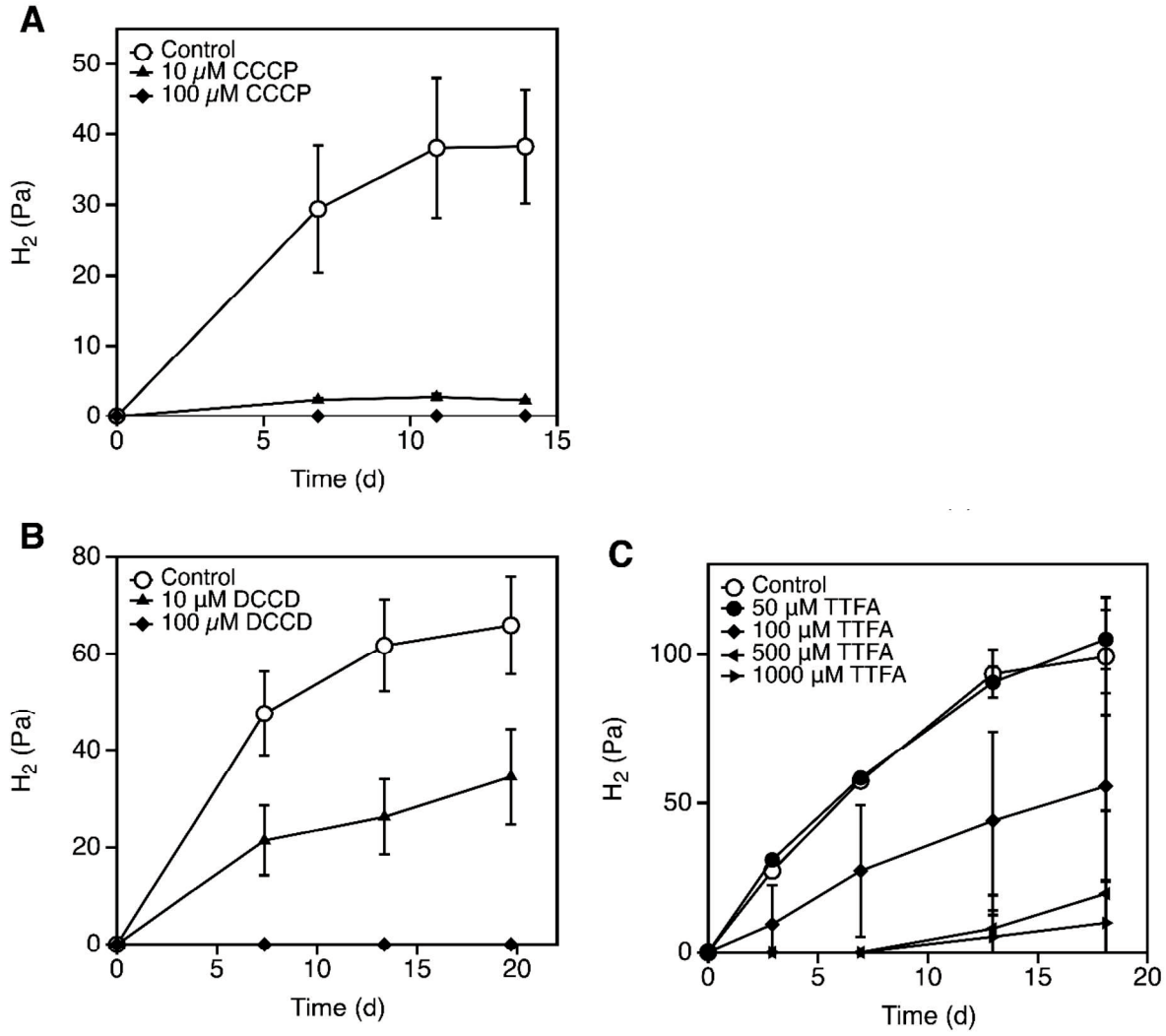

Fig. 1.5 Inhibitor effects on propionate hydrogen production by *P. thermopropionicum*.

The inoculated cells were washed before propionate incubation. Before the chemicals were added, a gas exchange was conducted. At a final concentration of 15.5 mM, pyridine was used as an inhibitor solvent and as a control. The inhibitors used were (A) carbonyl cyanide mchlorophenylhydrazone (CCCP), (B) N,N-dicyclohexylcarbodiimide (DCCD), and (C) 2-thenoyltrifluoroacetone (TTFA). The error bars represent the standard deviations for each of the three samples.

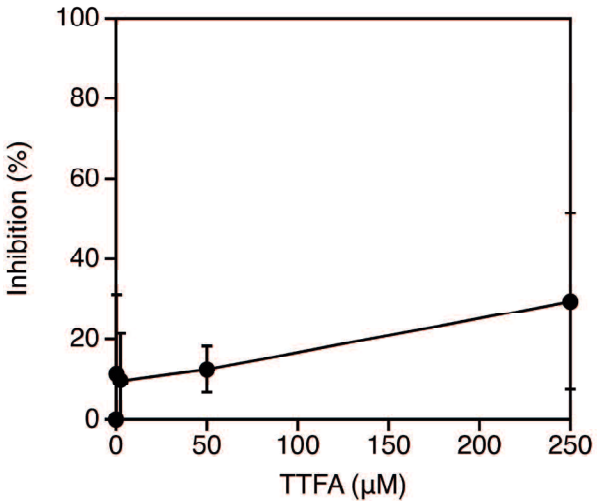

Fig. 1.6 TTFA inhibition on SDH activity in membrane fractions.

The succinate:Q_1 oxidoreductase activity was measured with the addition of 0.25, 2.5, 50, and 250 μM 2-thenoyltrifluoroacetone (TTFA). TTFA was dissolved in dimethyl sulfoxide and added to the reaction mixture before the addition of succinate to initiate the reaction. Percentage inhibition was calculated on the basis of activity values under 0 μM TTFA conditions. The error bars indicate the standard deviations of the three individual samples.

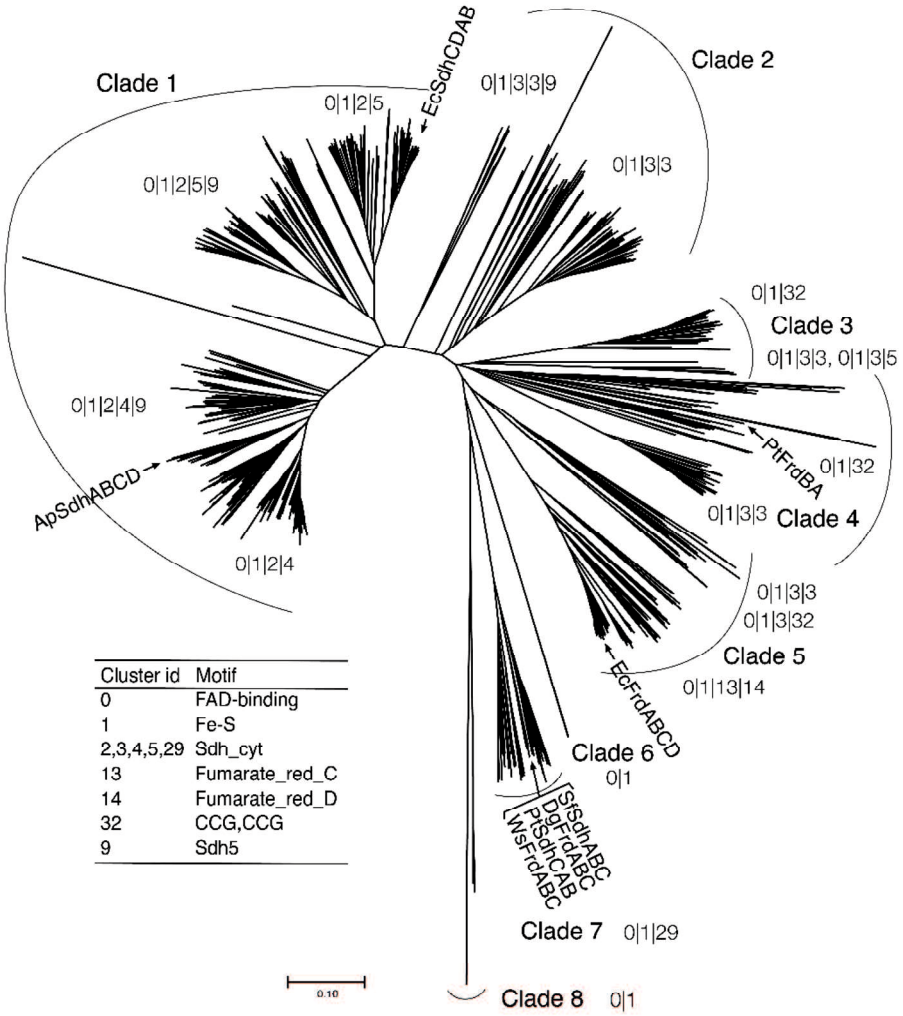

Fig. 1.7 Unrooted neighbor-joining phylogenetic tree of flavoprotein subunits of succinate dehydrogenase/fumarate reductase. A phylogenetic tree of 1,146 homologous protein sequences was constructed using the MEGAX 10.1.8 software package (Tamura et al., 2007; Stecher et al., 2020). The bar on the scale represents 0.1 substitutions per site. Each clade number is listed in Table S3. The numbers, which are cluster IDs, separated by "|" attached to each clade indicate the gene cluster structure in the clade containing each flavoprotein. The inset table displays the cluster ID as well as specific protein motifs listed in Table S4. Gene clusters were found in the strains depicted by the arrows: ApSdhCDAB, *Acetobacter 21asteurianus*; EcSdhCDAB, EcFrdABCD, *Escherichia coli*; PtFrdAB (SDH2), PtSdhCAB (SDH1), *Pelotomaculum thermopropionicum*; SfSdhCAB, *Syntrophobacter fumaroxidans*; DgFrdCAB, *Desulfovibrio gigas*; and WsFrdCAB, *Wolinella succinogenes*.

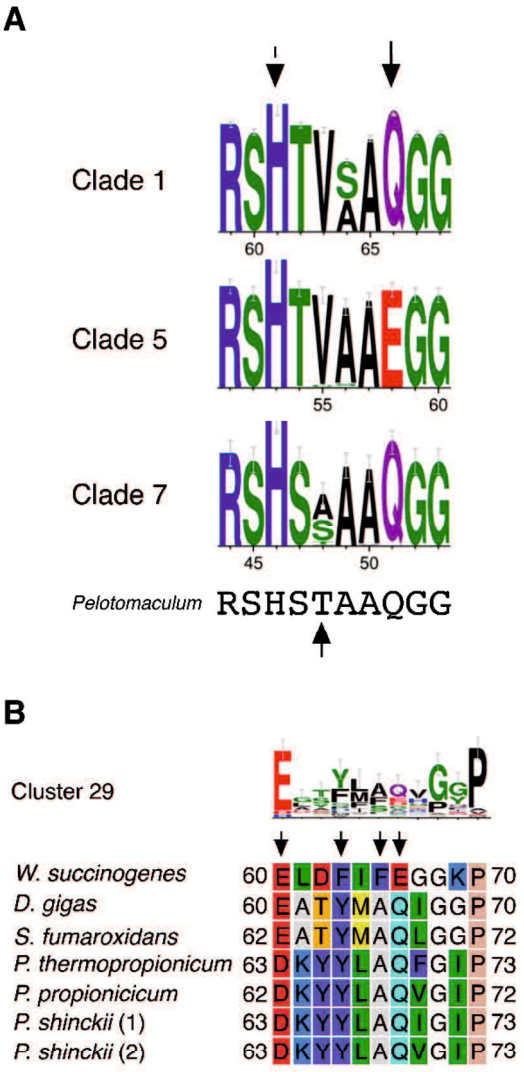

Fig. 1.8 Conserved regions in constructed alignments.

The logos depicted are (A) FAD-binding motifs for clades 1, 5, 7, and *Pelotomaculum* or (B) the putative menaquinone-binding site of cluster 29 containing the SdhC subunit. These logos were created using Weblogo (http://weblogo.berkeley.edu) and the alignment dataset shown in Fig. 1.5 or Fig. 1.7. The illustrated alignment was partially reconstructed from Fig. 1.7.

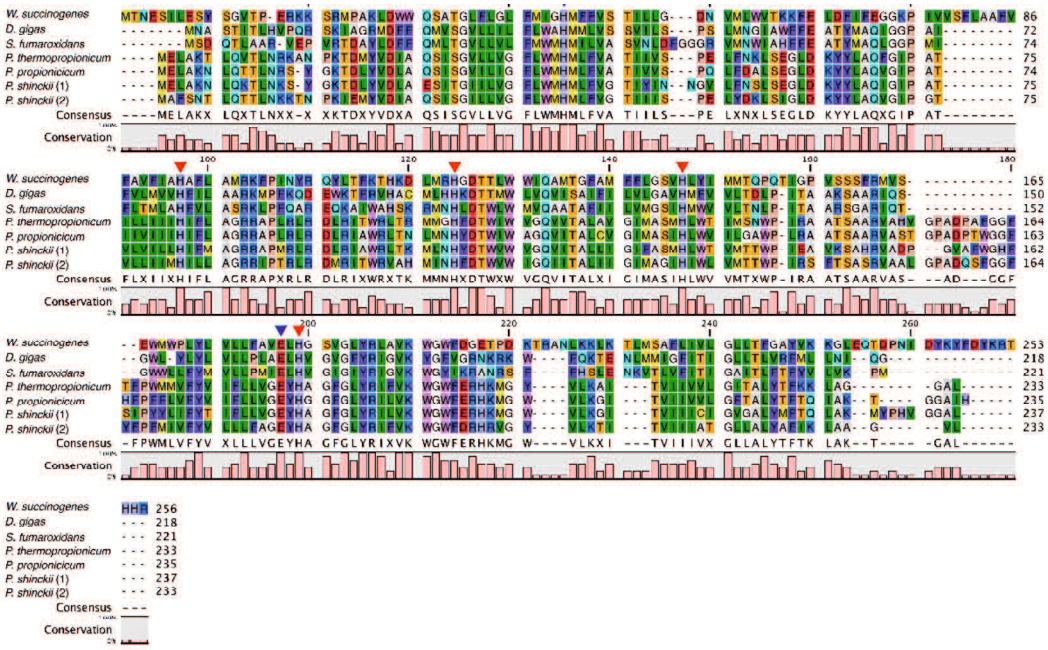

Fig. 1.9 Multiple alignments of cytochrome b subunits of succinate dehydrogenase/fumarate reductase belongs to cluster 29 from several microorganisms involved in clade 7 of the classification of flavoprotein subunit.

The alignment was generated using Clustal Omega 1.2.0 with default parameters in CLC Main Workbench 20.0.4 (http://www.Clcbio.com). UniProtKB accession of each sequence of a subunit from a specific strain is as follows: *W. succinogenes*, P17413; *D. gigas*, T2GAT5; *S. fumaroxidans*, *P. thermopropionicum*, A5D3J0; *P. propionicicum,* A0A4Y7RK43; *P. shinckii*, (1)A0A4Y7RCG7 (2)A0A4Y7RAL8. Red arrows indicate conserved histidine residues for heme binding. Blue arrows indicate conserved amino acid residues for E-pathway.

1.4 DISCUSSION

The present results suggest that the SDH of *P. thermopropionicum*, the key oxidizing enzyme directly related to propionate hydrogen production, localizes to the membrane and that the enzyme complex responsible needs to contain the membrane-integrated subunit. A sequence analysis predicted that SDH (SDH1) possesses a quinone pocket in SdhC (Table 1.1) and transfers electrons to menaquinone, corresponding to membrane-bound Q1 reductase activity (Table 1.2). In addition, we previously demonstrated that the expression levels of the genes encoding SDH1 (PTH_1016-1018) were higher than those of the genes encoding SDH2 (PTH_1492-1490) under conditions of syntrophic propionate oxidation[14]. These results indicate that SDH1 is primarily an SDH of *P. thermopropionicum*.

Furthermore, the results obtained herein revealed that SDH2 is a cytoplasmic FRD that receives electrons from NADH (Table 1.2), which is not associated with propionate oxidation. Therefore, we propose that sdh2A is frdA and sdh2B is frdB. The electrons required to reduce fumarate by FRD most likely originate from adjacent clustered PTH_1492 encoding multiple domains containing FrhB, which are the hydrogenase/dehydrogenase beta subunit of coenzyme F420, N terminus (IPR007516), coenzyme F420 hydrogenase/dehydrogenase beta subunit, C terminus (IPR007525), and 4Fe-4S ferredoxin-type iron-sulfur binding domain (IPR017896). However, an additional subunit that oxidizes NADH and transfers electrons to FRD may be required. In the genome of *P. thermopropionicum*, several genes exhibit possible NADH-oxidizing domains, such as NAD_binding_1 (Pfam No. PF00175), oxidized_FMN (PF00724), and Complex1_51K (PF01512). These domains containing genes include PTH_1405 (NAD_binding_1); PTH_0267, PTH_0595, and PTH_0596 (Oxidored_FMN); PTH_2011, PTH_1378, and PTH_2648 (Complex1_51K) (Table 1.3). The appropriate gene cannot be identified by the presence of a domain; however, the genes in *P. thermopropionicum* may be coupled to FRD. Furthermore, cytoplasmic FDRs are present in the syntrophic propionate-oxidizing bacterium *S. fumaroxidans* (Sfum_4092-4095, Sfum_1998-2000), which lacks heme groups and a predicted membrane-integrated domain cytoplasmic b-like[24].

The membrane-bound SDH of *P. thermopropionicum* required an ATP synthase-maintained membrane potential for succinate oxidation. This was necessary because propionate hydrogen production by *P. thermopropionicum* required a membrane potential (Fig. 1.5A), ATP synthase activity (Fig. 1.5B), and quinones (Fig. 1.5C). These results are consistent with the predicted reverse electron transport mechanism of membrane-bound SDH from the mesophilic propionate oxidizing bacterium, *S. wolinii*[11,15]. TTFA, which affects a broad range of quinone-associated proteins containing a quinone pocket[38], partially inhibited succinate:Q1 oxidoreductase activity (Fig. 1.6), suggesting that TTFA-causing reductions in SDH hydrogen production warrant further study. One possible TTFA target is the hydrogenase HYD4 because it includes the NrfD subunit, which accepts electrons from the quinone pool (Table 1.1). Additionally, membrane-bound NiFe-hydrogenase in *E. coli* requires a membrane potential[46]. The HYD4 of *P. thermopropionicum* showed significant homology with these

genes in *E. coli* (average of 54% positives), indicating that a membrane potential may also be required to drive the HYD4 reaction.

Membrane potential-requiring SDHs have been reported in *Bacillus subtilis*[47] and *Desulfovibrio* species[48]. Furthermore, the electrogenic catalysis of SDH has been demonstrated in *Bacillus licheniformis*[49]. The structure of the subunit and the reaction models of SDHs that utilize the membrane potential for succinate oxidation via transmembrane subunit C (cytochrome *b* subunit) have been proposed in SQR(SDH) of *B. licheniformis* and QFR(FRD) of *W. succinogene*[40,50,51]. In the *Wolinella* QFR, a compensatory proton transfer model via the E-pathway present in subunit C contributes an H+/e–ratio of 0.5 in the quinone-reducing reaction via succinate oxidation, whereas the H+/e–ratio is 1.0 in subunit C of *B. licheniformis* SQR, which does not utilize the E-pathway[40]. This difference in ratios in succinate-oxidizing reactions implies the energetic advantage of the E-pathway. *P. thermopropionicum* SdhC conserved several essential amino acid residues of the E-pathway (Fig. 1.9) and exhibited sufficient homology with the subunits of Desulfovibrio (33% identity) and Wolinella (27% identity). Subunit C of D. gigas QFR has been suggested to utilize the E-pathway in the reversible reaction of quinol oxidation[42]. These findings suggest that *P. thermopropionicum* SDH utilizes the E-pathway for succinate oxidation. Conversely, the binding of menaquinone to SdhC of *P. thermopropionicum* is crucial for the energetic efficiency of reactions in the SDHs of syntrophic propionate-oxidizing bacteria. Guan et al. (2018) proposed Q pockets, menaquinone-binding sites, and related amino acid residues based on the structure of subunit C of Desulfovibrio QFR. However, SdhC of *P. thermopropionicum* conserved these amino acid residues for heme binding in subunit C of *D. gigas* QFR (Fig. 1.9). Other residues associated with menaquinone binding in syntrophic propionate-oxidizing bacteria observed in the alignment (Fig. 1.7B) may be of greater importance for the menaquinone-specific interaction. These hypotheses require additional biological evidence.

According to the phylogenetic analysis of the flavoprotein subunit SdhA, syntrophic propionate-oxidizing bacteria highly clustered in clade 7 (Fig. 1.7). Since a correlation was observed between the classification of SdhA and that of the other subunits, SdhB, SdhC, and SdhD (Fig. 1.7), it is logical to assume that the relationship is significant. This hypothesis has been reported for the respiratory complex protein NADH:ubiquinone oxidoreductase (complex I)[52]. Additionally, the SdhA subunit is important for substrate specificity and is closely related to FAD binding. The FAD-binding motif in the homologs of SdhA suggests that clustered SdhA in clade 7 is a type of SDH, not FRD (Fig. 1.8A). These results indicate that the SDHs of syntrophic propionate-oxidizing bacteria have evolved specifically for these microorganisms and that the associated subunits play a crucial role in their function.

Hydrogen production from propionate oxidation in *P. thermopropionicum* requires a membrane potential, which is important for sustaining efficient methane fermentation. In addition, the efficiency of the energetic reaction of succinate oxidation needs to be considered in the structures of SdhA and

SdhC, particularly in syntrophic propionate-oxidizing bacteria. The biological mechanisms underlying energetically efficient propionate oxidation by the unique protein complexes of propionate-oxidizing bacteria will be elucidated by the accumulation of additional biological data, including those on actual cell and heterologous expression.

Table 1.3 Search of NADH oxidizing domain in *P. thermopropionicum*[a]

Query Pfam domain	Pfam No.	Query Length	Target locus Tag	Target UniProt Accession	Target Length	E-value	Score	Description	Related cluster	Trans-membrane[b]
NAD_binding_1	PF00175	109	PTH_1405	A5D2E4	280	3.1E-12	58.5	2-polyprenylphenol hydroxylase and related flavodoxin oxidoreductases	PTH_1405-1413	0
NAD_binding_1	PF00175	109	PTH_1180	A5D320	287	0.0009	31.3	2-polyprenylphenol hydroxylase and related flavodoxin oxidoreductases	?	0
Oxidored_FMN	PF00724	342	PTH_0267	A5D5M6	641	1.7E-81	285.8	Uncharacterized protein	?	0
Oxidored_FMN	PF00724	342	PTH_0595	A5D4R8	651	1.7E-60	216.8	NADH:flavin oxidoreductases	PTH_0594-0601	0
Oxidored_FMN	PF00724	342	PTH_0596	A5D4R7	649	4.6E-52	189.1	NADH:flavin oxidoreductases	PTH_0594-0601	0
Complex1_51K	PF01512	152	PTH_2011	A5D0Q3	551	5.4E-46	167.8	NADH:ubiquinone oxidoreductase, NADH-binding 51 kD subunit	HYD3 (PTH_2010-2012)	0
Complex1_51K	PF01512	152	PTH_2648	A5CYU7	617	1.9E-44	162.8	NADH:ubiquinone oxidoreductase, NADH-binding 51 kD subunit	PTH_2647-2650	0
Complex1_51K	PF01512	152	PTH_1378	A5D2H4	650	5.6E-43	158.0	NADH:ubiquinone oxidoreductase, NADH-binding 51 kD subunit	HYD2 (PTH_1377-1379)	0

[a]Search was performed by hmmsearch (https://www.ebi.ac.uk/Tools/hmmer/search/hmmsearch) with Pfam HMMs.

[b]Search was performed by DeepTMHMM (https://biolib.com/DTU/DeepTMHMM/)

1.5 PUBLICATION

This chapter represents an expanded version of the work originally published in: Tomoyuki Kosaka, Yuka Tsushima, Yusuke Shiota, Takayuki Ishiguchi, Kazuo Matsushita, Minenosuke Matsutani, and Mamoru Yamada, "Membrane Potential-requiring Succinate Dehydrogenase Constitutes the Key to Propionate Oxidation and Is Unique to Syntrophic Propionate-oxidizing Bacteria" Microbes and Environments, 2023 38(2) ME22111.
DOI: https://doi.org/10.1264/jsme2.ME22111

CHAPTER 2

Insight on flavinylation and functioning factor in Type B succinate dehydrogenase from Gram-positive bacteria

ABSTRACT

Succinate dehydrogenase (SDH), a multisubunit complex enzyme, catalyzes the oxidation of succinate to fumarate, coupled with quinone reduction. Maturation of each subunit and assembly of the complex is essential. However, little is known about the maturation mechanisms of SDH in Gram-positive bacteria. To elucidate the maturation of Type B SDH in Gram-positive bacteria, we heterologously expressed 3 SDH from *Bacillus subtilis*, *Corynebacterium glutamicum*, and *Pelotomaculum thermopropionicum* in *Escherichia coli*. The covalent binding of flavin adenine dinucleotide (FAD) at these SDH flavoprotein subunits was observed in heterologous expression as a complex. Their flavinylation was enhanced by the presence of the iron-sulfur subunit and fumarate. In contrast, the iron-sulfur subunit of heterologously expressed SDH without SDH activity showed no iron-sulfur clusters. These results suggest that during maturation of SDH, flavinylation is achieved by the complex and that other factors are required for the iron-sulfur cluster maturation.

2.1 INTRODUCTION

Succinate dehydrogenase (SDH) is conserved in all species from prokaryotes to eukaryotes and catalyzes the oxidation of succinate to fumarate coupled with quinone reduction[6]. Succinate oxidation is involved in the tricarboxylic acid cycle[8], the synthesis of precursors for lipid and amino acid metabolic pathways[9], a propionate oxidation pathway in propionate-oxidizing bacteria[10], and the membrane electron transport chain. Hence, SDH is central to a variety of cellular metabolic pathways and energy conversion in most organisms, and understanding how this enzymatic function is critical.

The membrane-associated and complex multisubunit SDH consists of 2 soluble subunits and membrane anchor subunit(s)[7]. The soluble flavoprotein subunit possesses a succinate oxidation catalytic site that involves covalently bonded flavin adenine dinucleotide (FAD) as a prosthetic group[53]. The iron-sulfur subunit, the other soluble subunit containing an iron-sulfur (Fe-S) cluster, mediates electron transfer from succinate to quinone, and the midpoint potentials of the Fe- S clusters favor electron transfer from FAD to quinone[54]. Membrane anchor subunit(s), composed of 1 or 2 subunits, possess quinone reduction sites containing 1 or 2 heme *b*. The membrane anchor subunit can be classified as Type A to F according to the number of constituent subunits, the number of transmembrane helices, the heme b they contain, and whether the quinone-binding sites are located proximally or distally to the soluble subunits[40,55]. For the SDH complex to function properly, oxidizing succinate and reducing quinone, the binding of FAD to the flavoprotein subunit, and the formation of Fe-S clusters on the iron-sulfur subunit are necessary. In addition, functional assembly of the SDH complex requires heme *b* in the membrane-anchoring subunits[56].

The covalent binding of FAD to the SDH flavoprotein subunit is called flavinylation and is essential for succinate oxidation because it increases the redox potential and allows electron transfer from succinate to FAD[41]. The co valent binding of FAD to the SDH flavoprotein subunit is mediated by an 8 α-N(3)-histidyl-FAD bond[53]. The flavinylation of the SDH flavoprotein subunit generally occurs before its assembly with other subunits in the complex[57]. The proportion of covalent binding of flavins, including FAD, to whole flavoproteins is approximately 10%, and the mechanism is suggested to be a self-catalytic protein modification[58]. However, the detailed mechanism of SDH flavinylation is not clear. Flavinylation of SDH flavoprotein subunits is enhanced by specific elements, including a FAD-binding protein, heat, and dicarboxylate[16,17,57,59-61]. The FAD-binding proteins SdhE, Sdh5, and SDHAF2 in bacteria, yeast, and humans, respectively, enhance the covalent binding of FAD to SDH flavoprotein subunits[59,60]. Dicarboxylate is necessary to maintain the structure of the flavoprotein and to synergize with SDHAF2 to properly orient flavin and SDHA[57,61]. Additionally, *Escherichia coli* SdhE increases the affinity for dicarboxylates[17]. The flavinylation of SDH flavoprotein subunits from hyperthermophilic Gram-negative bacteria and hyperthermophilic archaea, *Thermus thermophilus* and *Sulfolobus tokodaii*, which lack SdhE, requires heat and dicarboxylate[16]. Although many studies have reported the involvement of these elements in the flavinylation of flavoprotein subunits, only a few

have reported their involvement in certain organisms, such as Gram-positive bacteria, where conservation of the SdhE homolog is very low[18]. Interestingly, when the *Bacillus subtilis* sdhCAB operon is expressed in *E. coli*, the covalent binding of FAD in *B. subtilis* SDH flavoprotein subunit is not detected[62]. This suggests that host-specific elements are required for flavinylation in Gram-positive bacteria; however, these elements remain unclear. Multiple sequence analysis of the flavoprotein subunit of SDH/fumarate reductase (FRD), which has SDH activity, shows a high conservation of His required for FAD covalent bonding and Arg and His for dicarboxylic acid binding (Fig. 2.1 and 2.2). Finding out what elements are involved in the covalent binding of FAD to the flavoprotein subunit in the absence of c ha per ones such as SdhE should be interesting. Few reports have focused on flavinylation in Type B SDH from Gram-positive bacteria, which include propionate-oxidizing bacteria, with the exception of Actinobacteria.

In this study, to investigate the elements required for Type B SDH flavinylation in Gram-positive bacteria, we performed in vivo and in vitro flavinylation using 3 different heterologously expressed SDHs from Gram-positive bacteria: *B. subtilis*, a model organism; *Corynebacterium glutamicum*, an amino acid-producing bacterium widely used in industry; and *Pelotomaculum thermopropionicum*, a thermophilic propionate-oxidizing bacterium. This study provides insights into the flavinylation of Type B SDH from Gram-positive bacteria and information on the maturation of heterologously expressed SDHs.

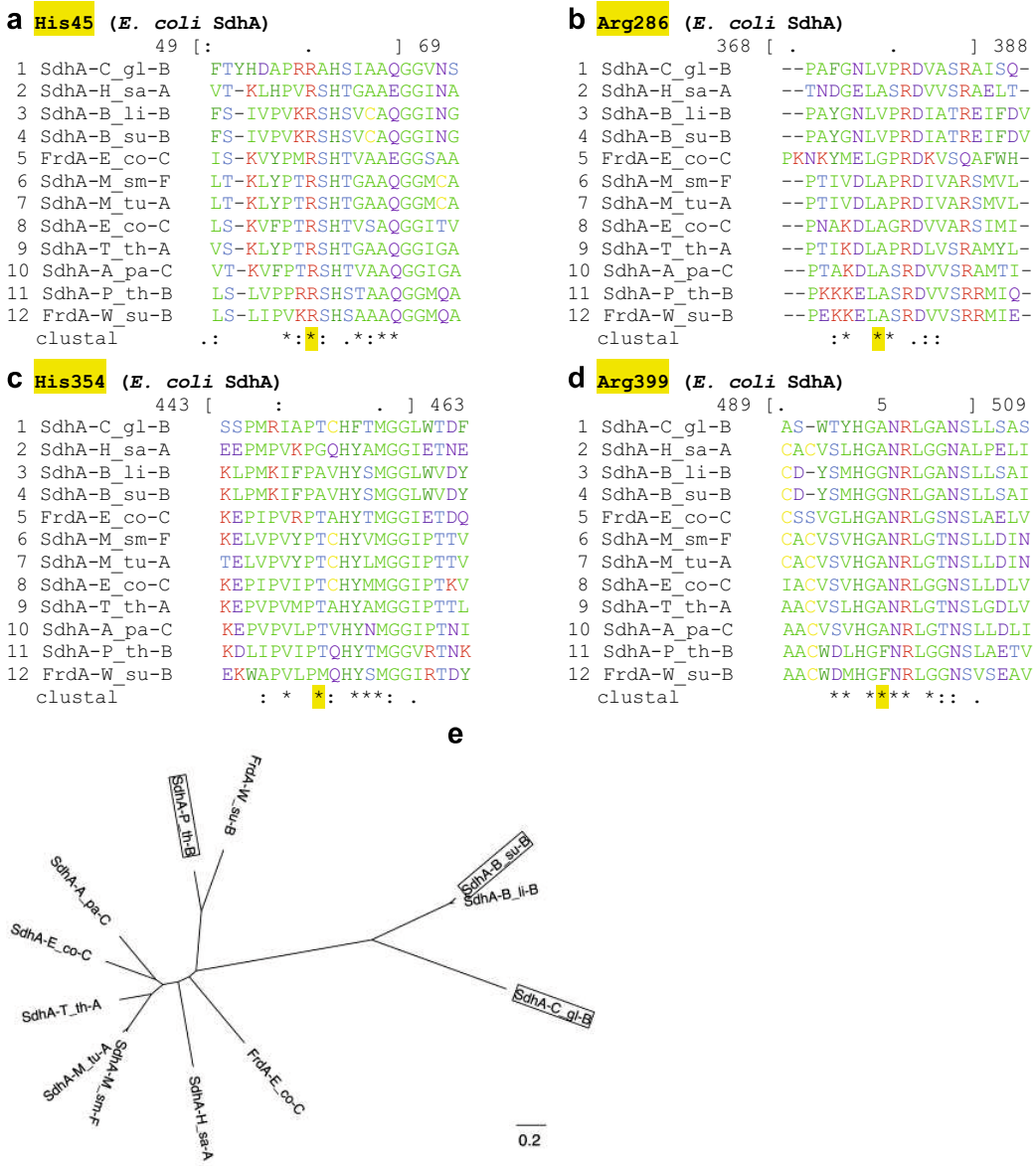

Fig. 2.1 The multiple alignment of the amino acid sequence of the homologs of SDH flavoprotein subunit was constructed using Muscle5 (Edgar 2022).

Used amino acid sequences were obtained from UniProt database (https://www.uniprot.org). The colored and separated alinement was produced by MView (Brown et al. 1998). The symbols in row "clustal" are * for full column identity, and : or . for strong and weak amino acid grouping, respectively. The list of tags for sequence information with the alignment is as follows: 1 SdhA-C_gl-B, *C. glutamicum* (UniProt accession: Q8NTD6, Type B); 2 SdhA-H_sa-A, *Halobacterium salinarum* (A0A4D6GU65, Type A); 3 SdhA-B_li-B, *Bacillus licheniformis* (T5HD13, Type B); 4 SdhA-B_su-B, *B. subtilis* (P08065, Type A); 4 FrdA-E_co-C, *E. coli* (P00363, Type C); 6 SdhA-M_sm-F, *Mycolicibacterium smegmatis* (A0A653FIT6, Type B); 7 SdhA-M_tu-A, *Mycobacterium tuberculosis* (L7N501, Type A); 8 SdhA-E_co-C, *E. coli* (P0AC41, Type C); 9 SdhA-T_th-A, *Thermus thermophilus* (Q5SIC0, Type A); 10 SdhA-A_pa-C, *Acetobacter pasteurianus* (C7JAR4, Type C); 11 SdhA-P_th-B, *P. thermopropionicum* (A5D3J1, Type B);

12 FrdA-W_su-B, *Wolinella succinogenes* (P17412, Type B). The type of SDH/FRD is based on the previous report[55]. (a) The alignment shows around His45 of SdhA of E. coli. (b) The alignment shows around Arg286. (c) The alignment shows around His354. (d) The alignment shows around Arg399. These residues are important for FAD-covalent binding[57] and dicarboxylic acid binding[63]. (e) The phylogenetic tree was subsequently generated by FigTree (http://tree.bio.ed.ac.uk/software/figtree/) using the distance data calculated by Clearcut program applying the relaxed neighbor-joining algorithm with the Kimura correction[64]. The scale bar corresponds to 0.1 substitutions per amino acid. The sequences used in this study are indicated as square.

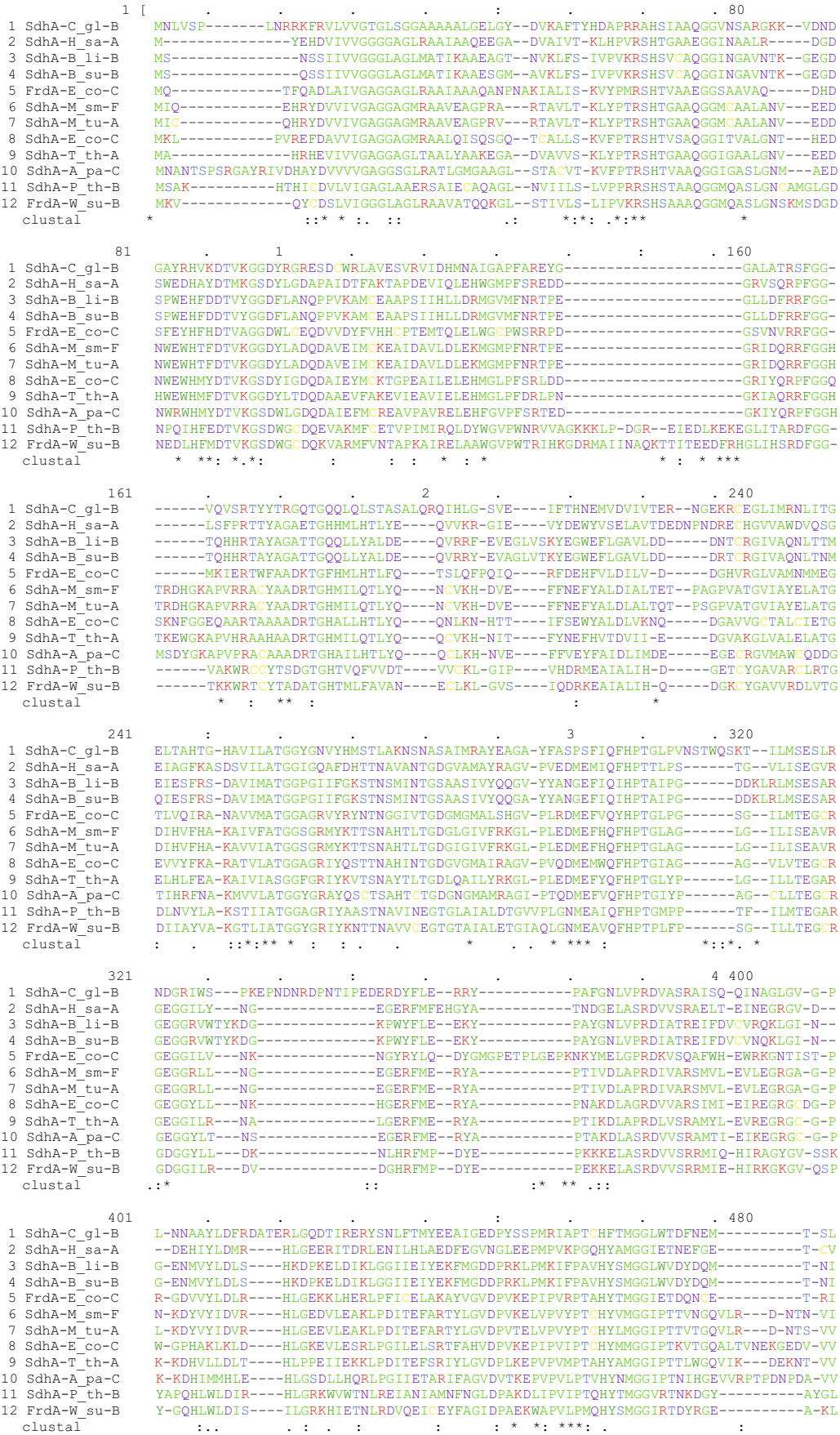
1 SdhA-C_gl-B
2 SdhA-H_sa-A
3 SdhA-B_li-B
4 SdhA-B_su-B
5 FrdA-E_co-C
6 SdhA-M_sm-F
7 SdhA-M_tu-A
8 SdhA-E_co-C
9 SdhA-T_th-A
10 SdhA-A_pa-C
11 SdhA-P_th-B
12 FrdA-W_su-B
clustal

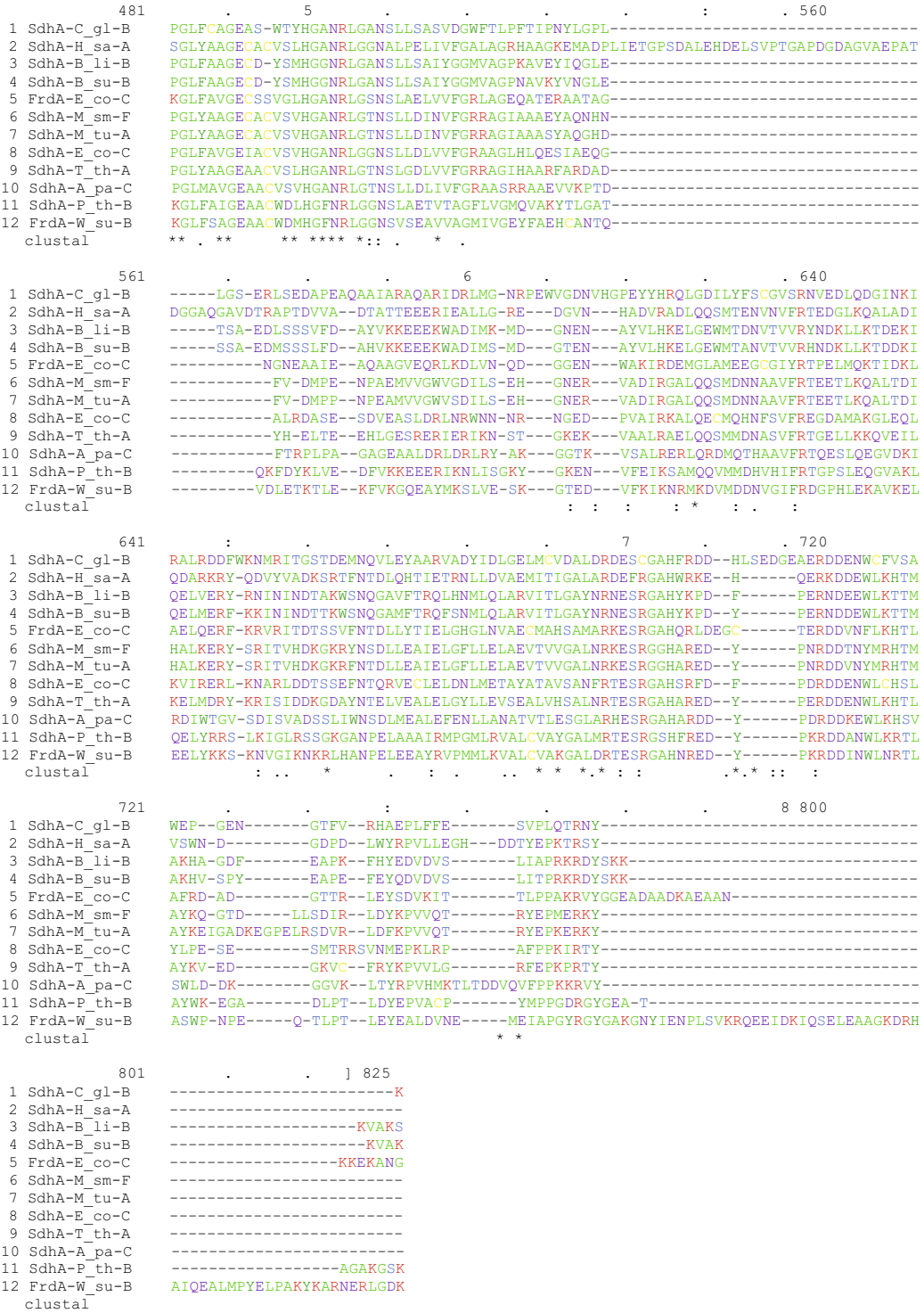

Fig. 2.2 The complete multiple sequence alignment of Fig. S1, which uses parts of it.

2.2 MATERIALS AND METHODS

2.2.1 Construction of *E. coli* strains and plasmids with disrupted genes

The constructed strains, plasmids, and primers are listed in Tables 2.1 and 2.2. Tks Gflex™ DNA polymerase (Takara Bio, Shiga, Japan) was used for DNA amplification. Disrupted strains were constructed from *E. coli* C41(DE3). The disruption of the *sdhCDAB* operon was performed using the one-step gene inactivation method[65], which resulted in *E. coli* Δsdh. Genomic DNA preparation for cloning SDH genes from *E. coli* BW25113 (sdhA; BW25113_0723, sdhB; BW25113_0724, sdhC; BW25113_0721, sdhD; BW25113_0722), SDH genes from *B. subtilis* 168 (sdhA; BSU_28440, sdhB; BSU_28430, sdhC; BSU_28450), and SDH genes from *C. glutamicum* ATCC13032 (sdhA; Cgl0371, sdhB; Cgl0372, sdhC; Cgl0370) was performed according to a general protocol for each microorganism, especially for SDH genes from *P. thermopropionicum* SI (sdhA; PTH_1017, sdhB; PTH_1018, sdhC; PTH_1016), which was performed as previously described[10]. Plasmids pBR322, pET23b, and pCA24N were used for cloning and gene expression analyses. The Gibson assembly[66] reaction mixture consisted of 10% PEG-8000, 0.25 M Tris-HCl pH 7.5, 20 mM MgCl2, 20 mM dithiothreitol, 40 μM dNTPs, 8 mU/μL T5 exonuclease (New England Biolabs, Ipswich, MA, USA), and 10 mU/μL Phusion polymerase (New England Biolabs, Ipswich, MA, USA) according to a previous report[67]. The Gibson assembly mixture was incubated with arbitrary DNA fragments for 30 min at 50 °C. After incubation, the reaction mixture was used to transform *E. coli* HST08.

2.2.2 Preparation of soluble and membrane fractions

Cells were cultivated in Luria Bertani (LB) medium containing 10 g/L NaCl, 10 g/L tryptone, and 5 g/L yeast extract. The constructed plasmids were transformed into *E. coli* Δsdh and the recombinant cells were grown overnight at 37 °C in LB medium plate containing 50 μg/mL ampicillin and 50 μg/mL kanamycin or 20 μg/mL chloramphenicol. A transformant colony was inoculated into 15 mL LB medium containing 50 μg/mL ampicillin and 50 μg/mL kanamycin or 20 μg/mL chloramphenicol and grown at 37 °C overnight with shaking at 150 rpm. Next, the 10 mL culture medium was inoculated into fresh 1 L LB medium containing 50 μg/mL ampicillin and 50 μg/mL kanamycin or 20 μg/mL chloramphenicol and grown at 30 °C for 24 h with shaking at 200 rpm. When using pET23b-based or pCA24N-based vectors, the protein expression was induced by 0.1 mM isopropyl β-D(-)-thiogalactopyranoside (IPTG). After 4-h incubation at 30 °C at 200 rpm, IPTG was added and the cells were incubated at 20 °C with shaking at 160 rpm for 18 h. The cells were then harvested by centrifugation at 6,000 rpm for 15 min at 4 °C, and the cell pellet was washed with an 8.5 g/L NaCl solution. Harvested cells were stored in an ultra-low temperature freezer at -80°C and collected in the quantities required for purification. The pellet exceeding 1.5 g wet weight was used and resuspended in an approximately 4-fold volume of 10 mM potassium phosphate buffer (pH 7.0). The cells were disrupted with a French pressure cell (American Instrument Company, USA) at 160,00 psi, and the

cell lysate was obtained by centrifugation (himac CP80WX; Hitachi, Tokyo, Japan) at 9,000 rpm for 15 min at 4 °C. The supernatant was subjected to ultra-centrifugation at 33,200 rpm for 90 min at 4 °C. The precipitate and supernatant fractions were separated and used as sources of the membrane and soluble fractions, respectively. The precipitate was suspended with 10 mM potassium phosphate buffer containing 2% Triton X-100 to a concentration of approximately 10 mg of protein per ml. The mixed solution was stirred at 40 rpm overnight at 4 °C. The mixture was then subjected to ultra-centrifugation at 40,300 rpm for 60 min at 4 °C and the supernatant was collected as the solubilized membrane fraction.

2.2.3 Protein purification

The soluble and solubilized membrane fractions were applied to a HisTrap™ HP column (Cytiva, USA) using AKTA™ prime plus (Cytiva, USA) with 20 mM sodium phosphate equilibration buffer at pH 7.4. The proteins were eluted using an imidazole concentration gradient from 20 to 500 mM. Selected elution fractions were applied to a PD-10 column (Cytiva, USA) and equilibrated with 10 mM potassium phosphate buffer (pH 7.0). The buffer contained 0.10% Triton X-100 for purification of membrane-associated proteins. Protein concentration was determined using the Pierce BCA Protein Assay Kit (Thermo Scientific, Waltham, MA, USA) according to the manufacturer's instructions.

2.2.4 Enzyme assays

SDH activity was measured by reduction of 2,6-dichloroindophenol (DCIP) or ubiquinone-1 (Q_1) as an electron acceptor. Succinate-dependent DCIP reduction was measured at 600 nm using a spectrophotometer (UV-1850; Shimadzu, Kyoto, Japan) at room temperature in a 3-mL plastic cuvette. The reaction mixture contained 16.6 mM potassium phosphate buffer (pH 7.0), 0.2 mM phenazine methosulfate, 0.11 mM DCIP, 8 mM sodium azide, and 20 mM succinate. The molecular extinction coefficient of DCIP was considered 14.52 mM^{-1} cm^{-1} [28] and one unit of activity corresponded to a reduction of 1 µmol DCIP min^{-1}. Succinate-dependent Q_1 reduction was measured at 275 nm using a spectrophotometer at room temperature in a 1-mL quartz cuvette. Dimethyl sulfoxide was used as the solvent for Q_1. The reaction solution contained 45.75 mM potassium phosphate buffer (pH 7.0), 8 mM sodium azide, 25 µM Q_1, and 20 mM succinate. The molecular extinction coefficient of Q_1 was considered 12.25 mM^{-1} cm^{-1} [29] and one unit corresponded to a reduction of 1 µmol Q_1 min^{-1}.

2.2.5 SDS-PAGE and in-gel FAD fluorescence detection

The purified sample was suspended in sample buffer containing 62.5 mM Tris-HCl pH 6.8, 2% SDS, 4% sucrose, and 0.002% bromophenol blue and incubated at 100 °C for 5

min. The incubated samples were subjected to SDS-PAGE on a 12% acrylamide gel. The molecular maker WIDE-VIEW™ Pre-stained Protein Size Marker III (Wako, Tokyo, Japan) was used. Proteins in the gel were stained with Coomassie brilliant blue (CBB). In-gel FAD fluorescence was detected by irradiation at 306 nm and 365 nm with a dual UV transilluminator (UVA-15; astec, Fukuoka, Japan) or irradiation at 470 nm with a blue light transilluminator (LED100; AMZ System Science, Osaka, Japan). Before UV irradiation, unstained gels were washed with pure water for 10 min and then incubated with 10% acetic acid at pH 3 for 15 min to oxidize the flavins. ImageJ software (National Institutes of Health, Bethesda, MD, USA) was used to quantify fluorescence intensity. The amount of estimated flavinylation was calculated as the intensity of FAD fluorescence divided by the intensity of CBB staining.

Table 2.1 Strains and plasmids used in this study

Strains	Description	Source
E. coli C41(DE3)	Effective strain for expression of membrane-associated proteins. F – ompThsdSB (rB- mB-) gal dcm (DE3)	Sigma-Aldrich
E. coli Δsdh	The prarent starin is C41 (DE3). ΔsdhCDAB::KmR	This study
E. coli HST08	F+ , *endA1* , *supE44* , *thi-1* , *recA1* , *relA1* , *gyrA96* , *phoA* , Φ80d*lacZ* ΔM15, Δ(*lacZYA* -*argF*)U169, Δ(*mrr* -*hsdRMS* -*mcrBC*), Δ*mcrA* , λ+	Takara
Plasmids	**Description**	**Source**
pBR322	Commonly used E. coli vector plasmid. Amp^R	Lab stock
pET23b	Commonly used IPTG-inducible gene expression vector plasmid containing T7 promoter. Amp^R	Lab stock
pCA24N	Commonly used IPTG-inducible gene expression vector plasmid containing T5 promoter. Cm^R	Lab stock
pKD20	Red recombinase expression plasmids.	Lab stock
pKD13	This plasmid contains the R6Kγ origin of replication and used to amplify the kanamycin resistance gene.	Lab stock
pBR-Ecsdh	pBR322-based plasmids. Regulates transcription of the *E. coli sdhCDAB* operon at the *E. coli sdhC* promoter. Histag is fused to the N-terminus of *sdhA* .	This study
pBR-Cgsdh	pBR322-based plasmids. Regulates transcription of the *C. glutamicum sdhCAB* operon at the *E. coli sdhC* promoter. Histag is fused to the N-terminus of *sdhA* .	This study
pBR-Bssdh	pBR322-based plasmids. Regulates transcription of the *B. subtilis sdhCAB* operon at the *E. coli sdhC* promoter. Histag is fused to the N-terminus of *sdhA* .	This study
pBR-Ptsdh	pBR322-based plasmids. Regulates transcription of the *P. thrmopropiouicum sdhCAB* operon at the *E. coli sdhC* promoter. Histag is fused to the N-terminus of *sdhA* .	This study
pET-EcsdhA	pET23b-based plasmids. Regulates transcription of the *E. coli sdhA* at the T7 promoter. Histag is fused to the N-terminus of *sdhA* .	This study
pET-CgsdhA	pET23b-based plasmids. Regulates transcription of the *C. glutamicum sdhA* at the T7 promoter. Histag is fused to the N-terminus of *sdhA* .	This study
pET-BssdhA	pET23b-based plasmids. Regulates transcription of the *B. subtilis sdhA* at the T7 promoter. Histag is fused to the N-terminus of *sdhA* .	This study
pET-PtsdhA	pET23b-based plasmids. Regulates transcription of the *P. thrmopropiouicum sdhA* at the T7 promoter. Histag is fused to the N-terminus of *sdhA* .	This study
pCA-BssdhA	pCA24N-based plasmids. Regulates transcription of the *B. subtilis sdhA* at the T5 promoter. Histag is fused to the N-terminus of *sdhA* .	This study
pCA-EcsdhB	pCA24N-based plasmids. Regulates transcription of the *E. coli sdhB* at the T5 promoter. Histag is fused to the N-terminus of *sdhB* .	This study
pCA-CgsdhB	pCA24N-based plasmids. Regulates transcription of the *C. glutamicum sdhB* at the T5 promoter. Histag is fused to the N-terminus of *sdhB* .	This study
pCA-BssdhB	pCA24N-based plasmids. Regulates transcription of the *B. subtilis sdhB* at the T5 promoter. Histag is fused to the N-terminus of *sdhB* .	This study
pCA-PtsdhB	pCA24N-based plasmids. Regulates transcription of the *P. thrmopropiouicum sdhB* at the T5 promoter. Histag is fused to the N-terminus of *sdhB* .	This study
pCA-CgsdhC	pCA24N-based plasmids. Regulates transcription of the *C. glutamicum sdhB* at the T5 promoter. Histag is fused to the C-terminus of *sdhC* .	This study
pCA-BssdhC	pCA24N-based plasmids. Regulates transcription of the *B. subtilis sdhB* at the T5 promoter. Histag is fused to the C-terminus of *sdhC* .	This study
pCA-PtsdhC	pCA24N-based plasmids. Regulates transcription of the *P. thrmopropiouicum sdhB* at the T5 promoter. Histag is fused to the C-terminus of *sdhC* .	This study

Table 2.2 Primer set used in this study

Primers	Sequence (5'→3')	PCR product
pKD13-Km-F	GTAGTCCCCAGGGAATAATAAGAACAGCATGTGGGCGTTATTCGTGTAGGCTGGAGCTGCTTC	Kanamycin resistance gene cassette for disruption of the *E.coli sdhCDAB* operon.
pKD13-Km-R	GCGCGTCTTATCAGGCCTACGGTTTACGCATTACGTTGCAACAAATTCCGGGGATCCGTCGAC	
pBR322-vector-F	ACGCCGGACGCATCGTG	pBR322 vector fragment for Gibson assembly with sdh operon.
pBR322-vector-R	ACAGGACGGGTGTGGTC	
EcsdhCDAB-F	GACCACACCCGTCCTGTTTAAGGTCTCCTTAGCGCCTTTATTGC	*E. coli* sdhCDAB operon containing *sdhC* promoter region fragment for Gibson assembly with pBR322.
EcsdhCDAB-R	CACGATGCGTCCGGCGTGTGATCCCTTAAGCATCTTTTTTATGCTTACTT	
EcsdhA-Nter-Histag-F	TGTGATGCACCATCACCATCACCATAAATTGCCAGTCAGAGAATTTGA	Plasmid fragment with histag fused to the N-terminus of the *E. coli sdhA* in pBR322.
EcsdhA-Nter-Histag-R	CAATTTATGGTGATGGTGATGGTGCATCACACACCCCACACCAC	
pBR-EcSdhCp-vector-F	TAAACCGTAGGCCTGATAAGACGC	pBR322 vector fragment containing *E. coli sdhC* promoter for Gibson assembly.
pBR-EcSdhCp-vector-R	CATGCTGTTCTTATTATTCCCTGGGG	
CgsdhCAB-F	GTCCCCAGGGAATAATAAGAACAGCATGACTGTTAGAAATCCGGACCGT	*C. glutamicum sdhCAB* operon fragment for Gibson assembly with pBR322.
CgsdhCAB-R	CGCGTCTTATCAGGCCTACGGTTTAGTCGTCTTTGCCTCGGAAAGC	
CgsdhA-Nter-Histag-F	AATTTATGCACCATCACCATCACCATAGCACTCACTCTGAAACCAC	Plasmid fragment with histag fused to the N-terminus of the *C. glutamicum sdhA* in pBR322.
CgsdhA-Nter-histag-R	GCTATGGTGATGGTGATGGTGCATAAATTCTTCCTAACCTTTACGCAATC	
BssdhCAB-F	GTCCCCAGGGAATAATAAGAACAGCATGTCTGGGAACAGAGAGTTTTATTTTCGA	*B. subtilis sdhCAB* operon fragment for Gibson assembly with pBR322.
BsdhCAB-R	TTGCGCGTCTTATCAGGCCTACGGTTTATACTCTGTCGCTTCCGAAGAAATTGC	
BssdhA-Nter-Histag-F	ATCATGCACCATCACCATCACCATAGTCAATCAAGCATTATCGTAGTCGGC	Plasmid fragment with histag fused to the N-terminus of the *B. subtilis sdhA* in pBR322.
BssdhA-Nter-histag-R	TTGACTATGGTGATGGTGATGGTGCATGATAGCCCCTCTCCCTCTAGT	
PtsdhCAB-F	GGGAATAATAAGAACAGCATGGAACTTGCAAAGACATTACAGGTTACATTAAAC	*P. thmropropionicum sdhCAB* operon fragment for Gibson assembly with pBR322.
PtsdhCAB-R	ATCAGGCCTACGGTTTACGATACTTTGAAACCTTTCAAGTCGAG	
PtsdhA-Nter-Histag-F	GTAGTGCACCATCACCATCACCATAGCGCAAACATACCCACATATGT	Plasmid fragment with histag fused to the N-terminus of the *P. thmropropionicum sdhA* in pBR322.
PtsdhA-Nter-histag-R	TGCGCTATGGTGATGGTGATGGTGCACTACAGGGCACCTCCCGC	
pET23b-vector-Nter-histag-F	TGAGATCCGGCTGCTAACAAAGC	pET23b vector fragment containing N-terminal His-tag of target protein for Gibson assembly.
pET23b-vector-Nter-histag-R	ATGGTGATGGTGATGGTGCATATGTATATCTCCTTCTTAAAGTTAAACAAAATTATTTCTAGAGGGA	
pET23b-vector-Cter-histag-F	CACCATCACCATCACCATTGAGATCCGGCTGCTAACAAAGC	pET23b vector fragment containing C-terminal His-tag of target protein for Gibson assembly.
pET23b-vector-Cter-histag-R	CATATGTATATCTCCTTCTTAAAGTTAAACAAAATTATTTCTAGAGGGA	
EcsdhA-pET23b-F	ATGCACCATCACCATCACCATAAATTGCCAGTCAGAGAATTTGATGC	*E. coli sdhA* fragment with Histag fused to the N-terminus for Gibson assembly with pET23b.
EcsdhA-pET23b-R	TTGTTAGCAGCCGGATCTCAGTAAGTACGAATCTTCGGCGGGA	
CgsdhA-pET23b-F	ATGCACCATCACCATCACCATAGCACTCACTCTGAAACCACCC	*C. glutamicum sdhA* fragment with Histag fused to the N-terminus for Gibson assembly with pET23b.
CgsdhA-pET23b-R	TTGTTAGCAGCCGGATCTCACTTGTAGTTCCTTGTCTGCAGTGGG	
BssdhA-pET23b-F	ATGCACCATCACCATCACCATAGTCAATCAAGCATTATCGTAGTCGG	*B. subtilis sdhA* fragment with Histag fused to the N-terminus for Gibson assembly with pET23b.
BssdhA-pET23b-R	TTGTTAGCAGCCGGATCTCATTTCGCCACCTTCTTCTTCG	
PtsdhA-pET23b-F	ATGCACCATCACCATCACCATAGCGCAAAACATACCCACATATGT	*P. thmropropionicum sdhA* fragment with Histag fused to the N-terminus for Gibson assembly with pET23b.
PtsdhA-pET23b-R	TTGTTAGCAGCCGGATCTCATTTGCTACCTTTGGCGCC	
pCA24N-vector-Nter-histag-F	GCTTGGACTCCTGTTGATAGATCC	pCA24N vector fragment containing N-terminal His-tag of target protein for Gibson assembly.
pCA24N-vector-Nter-histag-R	ATGGTGATGGTGATGGTGCATAGTT	
pCA24N-vector-F	GCTTGGACTCCTGTTGATAGATCC	pCA24N vector fragment for Gibson assembly with *sdhC*.
pCA24N-vector-R	CATAGTTAATTTCTCCTCTTTAATGAATTCTGTGTG	
BssdhA-pCA24N-F	TAACTATGCACCATCACCATCACCATAGTCAATCAAGCATTATCGTAGTCGGC	*B. subtilis sdhA* fragment with Histag fused to the N-terminus for Gibson assembly with pCA24N.
BssdhA-pCA24N-R	CTATCAACAGGAGTCCAAGCTTATTTCGCCACCTTCTTCTTCGAGTAATC	
EcsdhB-pCA24N-F	ACTATGCACCATCACCATCACCATAGACTCGAGTTTTTCAATTTATCGCTATAACCC	*E. coli sdhB* fragment with Histag fused to the N-terminus for Gibson assembly with pCA24N.
EcsdhB-pCA24N-R	CTATCAACAGGAGTCCAAGCTTACGCATTACGTTGCAACAACATCG	
CgsdhB-pCA24N-F	CACCATCACCATCACCATAAACTTACACTTGAGATCTGGCGTCA	*C. glutamicum sdhB* fragment with Histag fused to the N-terminus for Gibson assembly with pCA24N.
CgsdhB-pCA24N-R	TGGATCTATCAACAGGAGTCCAAGCTTACGCAATCCAGCCAACAGCG	
BssdhB-pCA24N-F	CACCATCACCATCACCATAAACTTACACTTGAGATCTGGCGTCA	*B. subtilis sdhB* fragment with Histag fused to the N-terminus for Gibson assembly with pCA24N.
BssdhB-pCA24N-R	CTATCAACAGGAGTCCAAGCTTATACTCTGTCGCTTCCGAAGAAATTGC	
PtsdhB-pCA24N-F	CACCATCACCATCACCATGGACGCCAGTTAACATTATCAATCTTTCG	*P. thmropropionicum sdhB* fragment with Histag fused to the N-terminus for Gibson assembly with pCA24N.
PtsdhB-pCA24N-R	TGGATCTATCAACAGGAGTCCAAGCTTACGATACTTTGAAACCTTT	
CgsdhC-pCA24N-F	CATTAAAGAGGAGAAATTAACTATGACTGTTAGAAATCCCGACCG	*C. glutamicum sdhC* fragment for Gibson assembly with pCA24N.
CgsdhC-pCA24N-R	CTATCAACAGGAGTCCAAGCTTACGCAATCCAGCCAACAGCG	
BssdhC-pCA24N-F	CATTAAAGAGGAGAAATTAACTATGTCTGGGAACAGAGAGTTTTATTTTCGAAGA	*B. subtilis sdhC* fragment for Gibson assembly with pCA24N.
BssdhC-pCA24N-R	CTATCAACAGGAGTCCAAGCTTAAACAAATGCAAAAATCGCTTTTAAGCCTAC	
PtsdhC-pCA24N-F	ATTCATTAAAGAGGAGAAATTAACTATGGAACTTGCAAAGACATT	*P. thmropropionicum sdhC* fragment for Gibson assembly with pCA24N.
PtsdhC-pCA24N-R	CTATCAACAGGAGTCCAAGCCTACAGGGCACCTCCCGCAA	
CgsdhC-Cter-Histag-F	ATTGCGCACCATCACCATCACCATTAAGCTTGGACTCCTGTTGATAGATCCAG	Plasmid fragment with histag fused to the C-terminus of the *C. glutamicum sdhC* in pCa24N.
CgsdhC-Cter-Histag-R	AGCTTAATGGTGATGGTGATGGTGCGCAATCCAGCCAACAGCGA	
BssdhC-Cter-Histag-F	GCATTTGTTCACCATCACCATCACCATTAAGCTTGGACTCCTGTTGATAGATCCA	Plasmid fragment with histag fused to the C-terminus of the *B. subtilis sdhC* in pCA24N.
BssdhC-Cter-Histag-R	AGCTTAATGGTGATGGTGATGGTGAACAATGCAAAAATCGCTTTTAAGCCT	
PtsdhC-Cter-Histag-F	TGCCCTGCACCATCACCATCACCATTAGGCTTGGACTCCTGTTGATAGATC	Plasmid fragment with histag fused to the C-terminus of the *P. thmropropionicum sdhC* in pCA24N.
PtsdhC-Cter-Histag-R	AGCCTAATGGTGATGGTGATGGTGCAGGGCACCTCCCGCAAG	

2.3 RESULTS

2.3.1 In vivo flavinylation and SDH activity of heterologously expressed SDH

Flavinylation of flavoproteins of several bacteria is enhanced by the FAD-binding protein SdhE[60]. However, this FAD-binding protein has species specificity, because the heterologously expressed SDH from *Acetobacter pasteurianus* is not fully complemented in the acetic acid bacterium *Gluconobacter oxydans*, and SdhE from *A. pasteurianus* is required for its full maturation[68]. In addition, the SdhE homolog is not conserved in many Gram-positive bacteria, including *B. subtilis*, *C. glutamicum*, and *P. thermopropionicum*[18]. To confirm whether flavinylation occurred by self-catalysis in *E. coli* or was enhanced by *E. coli* SdhE, three Gram-positive bacterial SDH flavoprotein subunits with an N-terminal His tag were expressed in *E. coli* and purified using a HisTrap™ HP column (Fig. 2.3a). Fluorescence detection of covalently bound FAD in the flavoprotein subunit revealed that the flavoprotein subunit of *E. coli* showed FAD fluorescence, whereas the other flavoprotein subunits did not (Fig. 2.3).

Because the three subunits, flavoprotein, Fe-S cluster, and membrane anchor, are highly conserved in the genomes of several Gram-positive bacteria, we attempted to heterologously express all three subunits simultaneously in *E. coli*. When purification was attempted from the membrane fraction using *E. coli* Δsdh as a host, the SDH complexes from *E. coli* and *C. glutamicum*, but not from *B. subtilis* and *P. thermopropionicum*, could be obtained (Fig. 2.4a-c). In the case of *E. coli* C41(DE3) host, purified samples with identical SDH flavoproteins of *P. thermopropionicum* and *B. subtilis* were obtained, but that of *C. glutamicum* was not (Fig. 2.4d). The purified *C. glutamicum* SDH complexes, in which the presence of the flavoprotein subunit was confirmed, clearly showed the presence of the iron-sulfur subunit, whereas the membrane anchor subunits were scarce (Fig. 2.4a). Because SDH complexes are tagged at the N-terminus of the flavoprotein subunit used for purification, the presence of soluble subunits in the membrane fraction indicates proper membrane localization of the complex in E. coli, probably forming a correct complex. Succinate oxidation activity was not completely lost in the membrane fraction of *E. coli* Δsdh (Table 2.3) owing to the presence of FRD, which has a covalently bound FAD and possesses succinate oxidation activity[69]. The succinate oxidation activity of *C. glutamicum* SDH expressed in *E. coli* was greater than that of the *E. coli* wild type, and the purified *C. glutamicum* SDH complex also had succinate oxidation activity (Table 2.3). The DCIP reduction activity of the purified *C. glutamicum* SDH from *C. glutamicum* ATCC 13869 was 57.5 U/mg[70], whereas the purified *C. glutamicum* SDH from *E. coli* Δsdh in this study was 43.0 U/mg (Table 2.3). However, the Q1 reductase activity of the purified SDH complexes from *E. coli* Δsdh was significantly lower than the DCIP reductase activity. The Q1 reductase activity of the SDH complex of *E. coli* was 34% of the DCIP reductase activity and that of *C. glutamicum* was 2.6% (Table 2.3). These results suggest that the membrane anchor subunits were lost during the purification process, and the complex structure could not be maintained, resulting in a reduction in Q1 reductase activity. FAD

fluorescence, which was not observed when the SDH flavoprotein subunits were expressed alone (Fig. 2.3), was detected at the flavoprotein position in the *C. glutamicum* SDH complex purified from *E. coli* Δsdh and the population of covalently bound FAD was approximately 13% of purified *E. coli* SDH (Fig. 2.4a, Table 2.3).Weak FAD fluorescence was also observed at the flavoprotein position in the *B. subtilis* and *P. thermopropionicum* SDHs purified from *E. coli* C41(DE3), respectively, which are not deficient in SDH and FRD (Fig. 2.4d). However, no activity was observed in the purified *B. subtilis* and *P. thermopropionicum* SDHs (data not shown).

2.3.2 Heterologous expression and purification of iron-sulfur and membrane anchor subunits

FAD fluorescence at the flavoprotein position in the purified SDH complex was observed; however, heterologously expressed SDHs of *B. subtilis* and *P. thermopropionicum* did not function in *E. coli*. To analyze the maturation of each subunit, individual expression and purification of the N-terminally tagged iron-sulfur subunit and the C-terminally tagged membrane anchor subunit were performed. Purified proteins separated by SDS-PAGE showed identical bands corresponding to iron-sulfur and membrane anchor subunits, although the purified proteins contained many off-target proteins (Fig. 2.5). Exceptionally, the yield of *C. glutamicum* membrane anchor subunit was very low, and the band of the *C. glutamicum* membrane anchor subunit could not be identified. (Fig. 2.5b). The *B. subtilis* membrane anchor subunit was successfully expressed in *E. coli* and contained heme b_{558} [71]. Typical bacterial SDH iron-sulfur subunits possess one each of [2Fe-2S], [3Fe-4S], and [4Fe-4S] clusters. Additionally, the [3Fe-4S] and [4Fe-4S] clusters show a broad absorbance peak around 390-410 nm, which is difficult to distinguish. The presence of iron-sulfur cluster(s) can be inferred from the detection of the characteristic optical absorbance of iron-sulfur proteins[72]. The purified iron-sulfur subunits from *E. coli* and *C. glutamicum* showed a broad absorption peak around 410-420 nm, suggesting the presence of one or more iron-sulfur cluster(s), which were not observed in those from *B. subtilis* and *P. thermopropionicum* (Fig. 2.6).

2.3.3 *in vitro* flavinylation of *C. glutamicum* and *B. subtilis* SDHs

Our results indicate that flavinylation of the SDH flavoprotein subunit from the three Gram-positive bacteria used in this study was observed when the SDH complex was heterologously expressed, but not when expressed alone. To elucidate in more detail the flavinylation mechanism of SDH used in this study, in vitro flavinylation of the SDH flavoprotein subunit was performed using complex reconstruction. The purified membrane anchor subunit of *C. glutamicum* had a low yield (Fig. 2.5), and the purified subunit of *P. thermopropionicum* was degraded during the incubation for in vitro flavinylation (data not shown). Therefore, purified flavoprotein and iron-sulfur subunits of *C. glutamicum* and the corresponding purified subunits of *B. subtilis* were used. In vitro flavinylation of

the SDH flavoprotein subunit of *C. glutamicum* showed that slight FAD-covalent binding occurred in the presence of 100 μM FAD, and the binding was enhanced by the presence of fumarate or the iron-sulfur subunit. The amount of flavinylation increased approximately 4-fold in the presence of each (Fig. 2.7a lane 1-3). The concomitant addition of fumarate and iron-sulfur subunit did not result in a greater enhancement of flavinylation when compared with the presence of each component, and the amount of iron-sulfur subunit did not have a significant effect (Fig. 2.7a, lanes 4-8). Moreover, in vitro flavinylation of the SDH flavoprotein subunit of *B. subtilis* also showed slight FAD binding in the presence of 100 μM FAD and increased flavinylation in the presence of the *B. subtilis* iron-sulfur subunit (Fig. 2.7b, lanes 1 and 2). The presence of the iron-sulfur and membrane anchor subunits increased flavinylation approximately 1.5-fold compared to when only FAD was present (Fig. 2.7b, lane 3). No additional increase in flavinylation was observed in the presence of fumarate and Q1 when all subunits of *B. subtilis* were present (Fig. 2.7b, lanes 4-6).

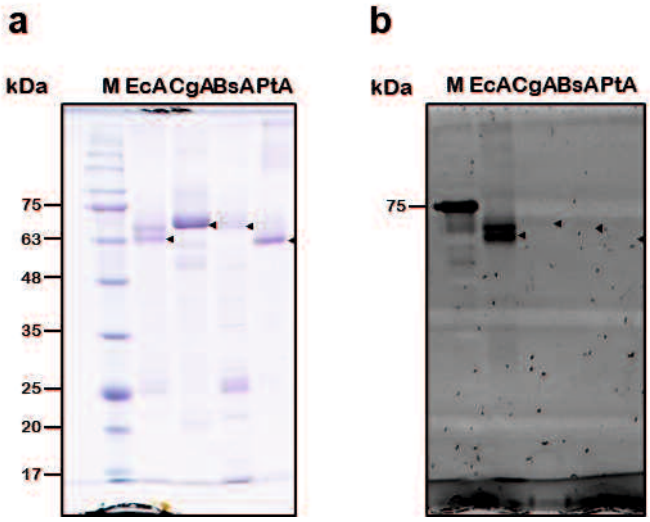

Fig. 2.3 Purification of SDH flavoprotein subunits from E. coli and detection of covalently bound FAD

SDH flavoprotein subunits were heterologously expressed using a pET23b-based vector in E. coli Δsdh and purified using a HisTrap™ HP column, then separated by SDS-PAGE. The arrows show each flavoprotein subunit. (a) CBB-stained. Each sample loaded 1 μg. (b) In-gel fluorescence of covalently bound FAD in flavoproteins before CBB staining. UV irradiation was used. These data represent results from three independent experiments. The approximate predicted molecular weight of the His-tag fusion flavoprotein subunit of each strain is as follows: *E. coli* (EcA), 65 kDa; *C. glutamicum* (CgA), 76 kDa; *B. subtilis* (BsA), 66 kDa; *P. thermopropionicum* (PtA), 67 kDa. M is the molecular marker. The molecular weight was predicted using Expasy (https://web.expasy.org/compute_pi/).

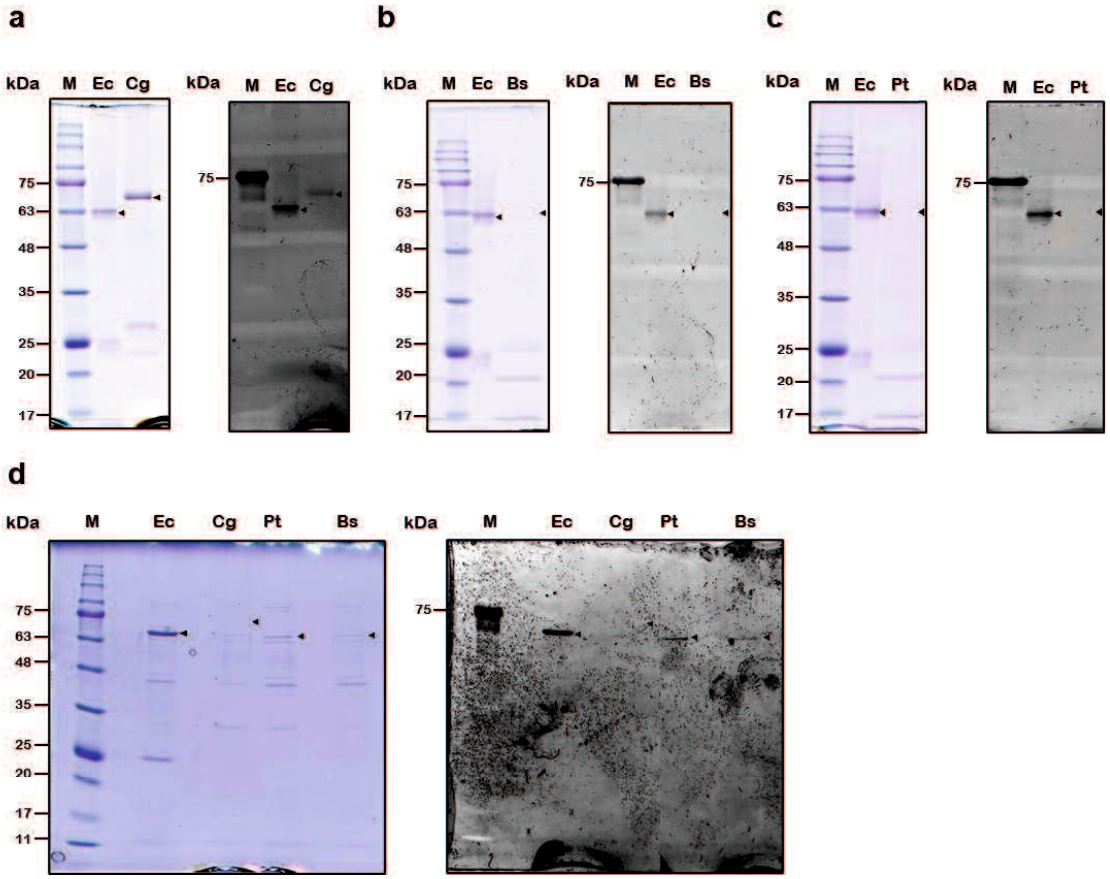

Fig. 2.4 Purification of SDH complexes from *E. coli* and detection of covalently bound FAD

SDH complexes were heterologously expressed using a pBR322-based vector and purified using a HisTrap™ HP column, then separated by SDS-PAGE. Each sample loaded 1 μg. The arrows show each flavoprotein subunit. Each left panel shows a CBB-stained gel and the right panel shows in-gel fluorescence of covalently bound FAD in the flavoprotein subunit before CBB staining. (a) *C. glutamicum* SDH complex heterologously expressed in *E. coli* Δsdh. (b) *B. subtilis* SDH complex heterologously expressed in *E. coli* Δsdh. (c), *P. thermopropionicum* SDH complex heterologously expressed in *E. coli* Δsdh. UV irradiation was used for in-gel fluorescence detection in panel a-c. Panels a-c each represent results from three independent experiments. (d) SDH complex heterologously expressed in *E. coli* C41(DE3). Blue light was used for in-gel fluorescence detection. These data were obtained from a single experiment. The gel image is joined by deleting the lane between Cg and Pt, but the size is not changed. Marker: molecular marker; Ec: *E. coli* SDH; Cg: *C. glutamicum* SDH; Bs: *B. subtilis* SDH; Pt: *P. thermopropionicum* SDH.

.

Table 2.3 Enzymatic activities and flavinylation of recombinant SDH heterologously produced in *E. coli*

	Membrane fraction	Purified sample		
	Succinate:PMS/DCIP oxidoreductase activity[a] (U/mg)	Succinate:PMS/DCIP oxidoreductase activity[a] (U/mg)	Succinate:Q1 oxidoreductase activity[a] (U/mg)	Flavinylation population[a] (%)
E. coli C41(DE3)	0.19 ± 0.03	-	-	-
Δsdh	0.02 ± 0.00	-	-	-
EcSdh/Δsdh	2.54 ± 0.29	21.1 ± 15.7	7.17 ± 3.95	100
CgSdh/Δsdh	0.73 ± 0.25	43.0 ± 8.6	1.12 ± 0.10	12.7 ± 2.21
BsSdh/Δsdh	0.01 ± 0.00	ND[b]	0.10 ± 0.17	ND
PtSdh/Δsdh	0.01 ± 0.00	ND	0.07 ± 0.08	ND

Ec: *E. coli*; Cg: *C. glutamicum*; Bs: *B. subtilis*; Pt: *P. thermopropionicum*. *± standard deviations (n = 3).

[b]ND means not detected.

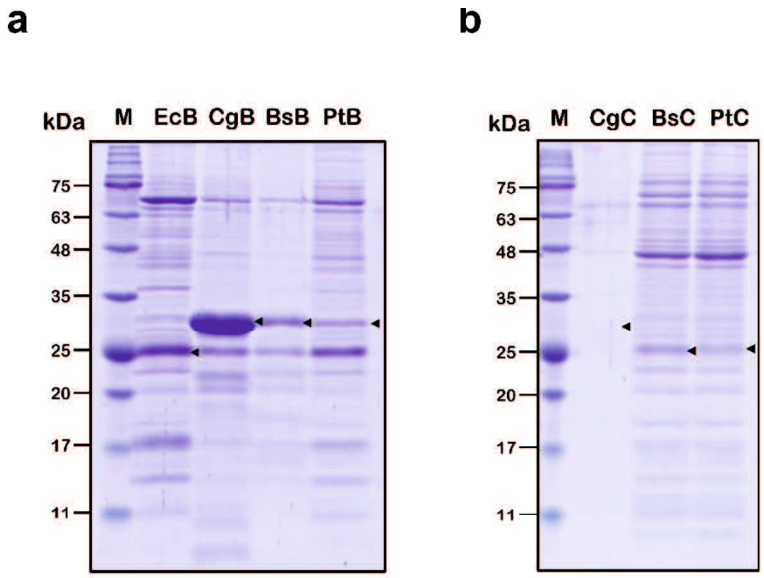

Fig. 2.5 Purification of heterologously expressed SDH iron-sulfur and membrane anchor subunits

Iron-sulfur cluster and membrane anchor subunits were heterologously expressed using a pCA24N-based vector in *E. coli*Δsdh and purified using a HisTrap™ HP column, then separated by SDS-PAGE stained by CBB. Each sample loaded 2 μg. (a) Iron-sulfur subunits. (b) Membrane anchor subunits. The arrows show each subunit. These data represent results from three independent experiments. The approximate predicted molecular weight of the His-tag fusion iron-sulfur subunit of each strain is as follows: *E. coli* (EcB), 28 kDa; *C. glutamicum* (CgB), 27 kDa; *B. subtilis* (BsB), 29 kDa; *P. thermopropionicum* (PtB), 29 kDa. The approximate predicted molecular weight of the His-tag fusion iron-sulfur subunit of each strain is as follows: *C. glutamicum* (CgC), 29 kDa; *B. subtilis* (BsC), 24 kDa; *P. thermopropionicum* (PtB), 27 kDa. M is the molecular marker. The molecular weight was predicted using Expasy (https://web.expasy.org/compute_pi/).

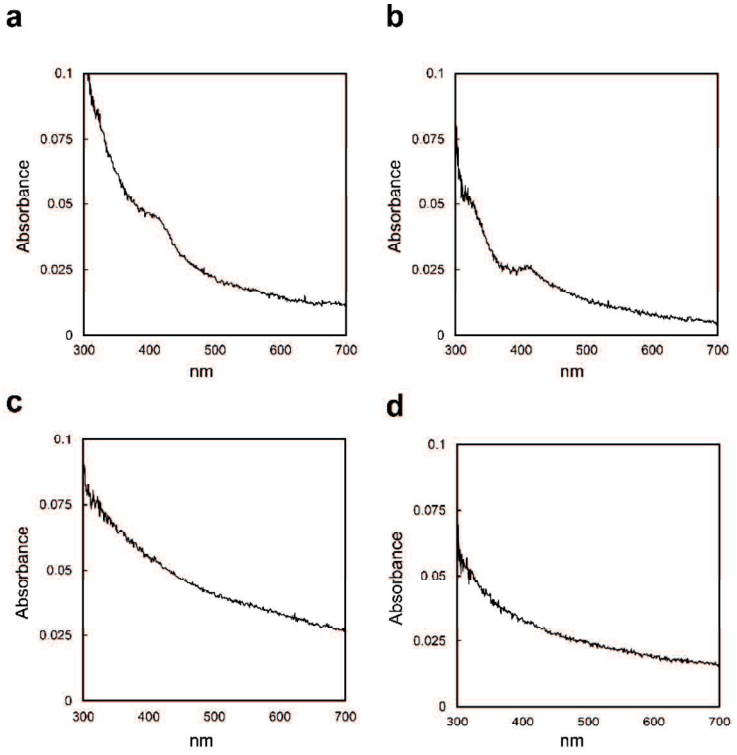

Fig. 2.6 Absorption spectra of purified iron-sulfur subunits

Measurements were performed using a UV-1800 (Shimadzu) instrument with the UVProbe program (Shimadzu). Spectra were recorded between 300 and 700 nm using a 1-mL quartz cuvette with a 10-mm path length. The baselines of the spectra were obtained by measuring in 10 mM potassium phosphate buffer. Protein concentrations were adjusted to 50 μg/mL. These data represent results from three independent experiments. (a) Absorption spectra of the iron-sulfur subunit of *E. coli*. (b) Absorption spectra of the iron-sulfur subunit of *C. glutamicum*. (c) Absorption spectra of the iron-sulfur subunit of *B. subtilis*. (d) Absorption spectra of the iron-sulfur subunit of *P. thermopropionicum.*

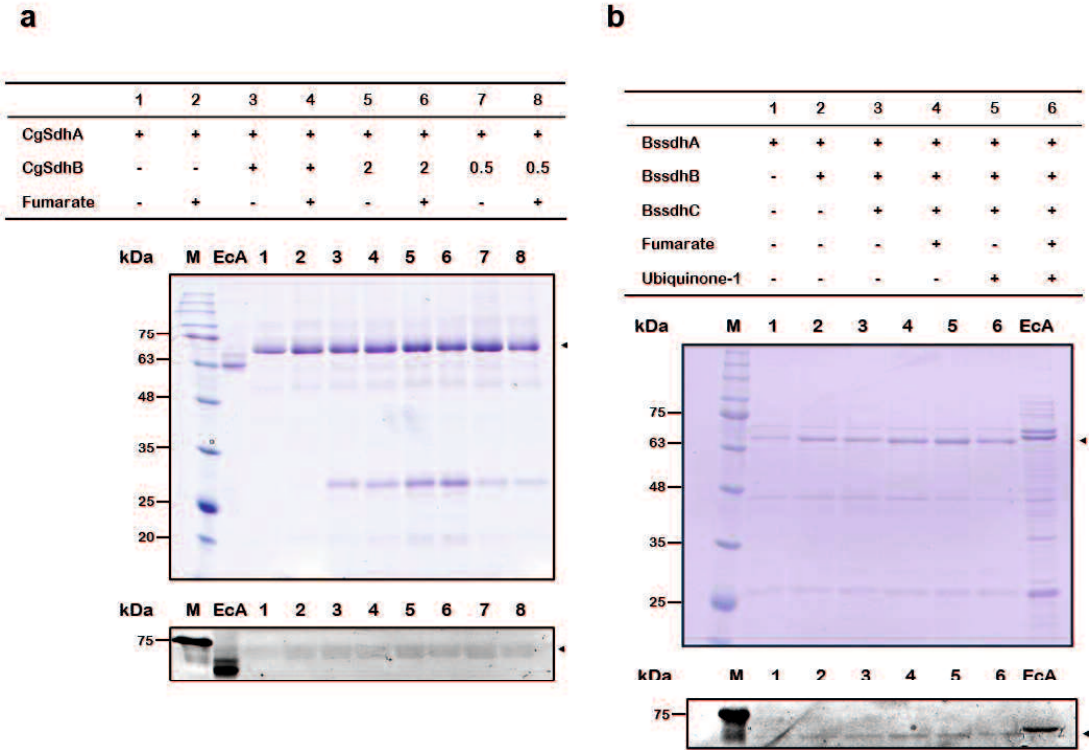

Fig. 2.7 ***In vitro*** **flavinylation of** ***C. glutamicum*** **and** ***B. subtilis*** **SDH flavoprotein subunits**

Approximately 1 μg of flavoprotein subunit, 0.5 μg of iron-sulfur subunit, 0.5 μg of membrane anchor subunit, 100 μM of FAD, 20 mM of fumarate, and 5 μM of Q_1 were incubated in 20 μL of 10 mM phosphate buffer (pH 7.0) at 30°C for 60 min. After incubation, all samples were suspended in sample buffer and in-gel fluorescence was determined as described in the experimental procedures. The top panel shows the conditions for each lane: +, presence; -, absence; 2, twice the amount (1 μg); 0.5, half the amount (0.25 μg). The middle panel shows the CBB-stained SDS-PAGE gel for each reaction mixture. The bottom panel shows the in-gel fluorescence of covalently bound FAD in the flavoprotein subunit before CBB staining. The arrows show each flavoprotein subunit. (a) *In vitro* flavinylation of *C. glutamicum* SDH flavoprotein subunit. Flavoprotein subunit and iron-sulfur subunit of *C. glutamicum* SDH were heterologously expressed using a pET23b-based vector in *E. coli* Δsdh and purified using a HisTrap™ HP column. UV irradiation was used for in-gel fluorescence detection. These data represent results from two independent experiments. (b) *In vitro* flavinylation of *B. subtilis* SDH flavoprotein subunit. Each subunit was heterologously expressed using a pCA24N-based vector in *E. coli* Δsdh and purified using a HisTrap™ HP column. Blue light was used for in-gel fluorescence detection. These data represent results from two independent experiments.

2.4 DISCUSSION

In this study, no fluorescence resulting from covalent binding of FAD was observed in the individual heterologous expression of three Type B SDH flavoprotein subunits from Gram-positive bacteria (Fig. 2.3). However, when expressed as part of the SDH complex, this fluorescence was observed in the *C. glutamicum* SDH flavoprotein subunit (Fig. 2.4a and 2.8), and the same was also suggested in the *B. subtilis* and *P. thermopropionicum* SDH flavoprotein subunits (Fig. 2.4d). These results indicate that flavinylation of the heterologously expressed Type B SDH flavoprotein subunits from three Gram-positive bacteria was neither self-catalyzed in the *E. coli* cell nor enhanced by *E. coli* SdhE, whereas flavinylation of the Type B SDH flavoprotein subunit was enhanced by the presence of other SDH subunits. Additionally, in vitro self-catalyzed flavinylation of the SDH flavoprotein subunit of *C. glutamicum* was enhanced by the presence of the iron-sulfur subunit or fumarate (Fig. 2.7a). Fumarate enhances flavinylation[17] and is an essential element for certain SDH flavinylation[16], suggesting that fumarate is related to the SDH flavinylation of a wide range of species. Furthermore, in vitro self-catalyzed flavinylation of the *B. subtilis* SDH flavoprotein subunits was enhanced in the presence of an iron-sulfur subunit, and further enhancement was observed in the presence of iron-sulfur and membrane anchor subunits. These in vitro self-catalyzed flavinylation suggest that the flavinylation of SDH used in this study was assisted not only by fumarate but also by the presence of an iron-sulfur subunit and that the presence of the membrane subunit may stabilize the structure of the complex, thereby enhancing flavinylation.

The self-catalyzed flavinylation of flavoproteins assisted by other subunits has been reported in p-cresol methylhydroxylase (PCMH), which catalyzes the oxidation of p-cresol to 4-hydroxybenzyl alcohol[73]. PCMH is composed of two flavoprotein subunits and two c-type cytochrome subunits and requires FAD as a prosthetic group; flavinylation of the flavoprotein subunit is self-catalyzed in the presence of a c-type cytochrome subunit[73]. In addition, flavinylation of the PCMH flavoprotein subunit is induced by small rearrangements in the flavoprotein-cytochrome interface region, which alters the conformation of the FAD-binding site[74]. Therefore, the flavinylation caused by self-catalysis and structural change may occur in the SDH of Gram-positive bacteria.

The mechanism of flavin re-oxidation and stabilization, where electrons move from the covalently bound flavin, such as FAD and flavin mononucleotide (FMN), to electron acceptors, is also an interesting one. Trimethylamine dehydrogenase (TMADH) contains covalently bound FMN and catalyzes the oxidation of trimethylamine N-demethylation. In TMADH, FMN is re-oxidized by transferring electrons to the Fe-S cluster, stabilizing the covalent bond[75]. In addition, the iron-sulfur subunit of SDH supports flavinylation but is not essential[76]. The results of in vitro flavinylation in *C. glutamicum* (Fig. 2.7a) are consistent with FAD being stabilized by its iron-sulfur cluster. Interestingly, we observed an increase in in vitro flavinylation of *B. subtilis* SDH by the iron-sulfur subunit, despite the absence of Fe-S clusters in this subunit (Fig. 2.6 and 2.7b), and this result is inconsistent with the

previous report[75]. One possibility is that in vitro flavinylation of the *B. subtilis* SDH flavoprotein stabilizes the covalent bond by re-oxidation through electron transfer to oxygen. This speculation is supported by evidence of electron transfer to oxygen during in vitro flavinylation of the *E. coli* SDH flavoprotein subunit[17].

This study provides the insight that the flavinylation of Type B SDH from Gram-positive bacteria is assisted by the presence of fumarate and an iron-sulfur subunit; however, the detailed flavinylation mechanism remains unclear, because the estimated population of flavinylated *C. glutamicum* SDH complex expressed in *E. coli* was lower than that of *E. coli* SDH complex (Table 2.3). Furthermore, the accumulation in the cytoplasm of flavinylated SdhA flavoprotein subunit in the *B. subtilis* iron-sulfur subunit deletion mutant strain[77] and the present results of Type B SDH complexes of Gram-positive bacteria expressed in *E. coli* strains harboring SdhE (and each subunit of FRD) may suggest the presence of a certain species-specific factor(s) other than fumarate and the iron-sulfur subunit. In these connections, we also noted that the estimation of the amount of flavinylation based on the in-gel FAD fluorescence method would require more attention, as the estimated amount of flavinylation of the E. coli SdhA flavoprotein subunit was roughly 1.8-fold of that of the *E. coli* SDH complex, under the same conditions when those of the flavinylated *C. glutamicum* SDH complex and SdhA flavoprotein were approximately 18% and negligible, respectively, than that of the *E. coli* complex (Fig. 2.8). Further analysis including biochemical experiments is therefore required to elucidate the detailed flavinylation mechanism of Type B SDH in vivo and to explore the additional species-specific element that assists flavinylation (e.g., chaperone protein).

Certain heterologously expressed enzymes are often inactive because of the incorrect conformation of components, wrong localization to the membrane, and lack of maturation of the cofactor-requiring subunit. We observed succinate oxidation activity of the purified SDH of *C. glutamicum* from *E. coli* cells (Table 2.3), which indicates the functional heterologous expression of SDH from Gram-positive bacteria. The characteristic absorption spectra of each iron-sulfur cluster are so close that distinguishing between them by absorption spectra is difficult. Consequently, accurate identification of iron-sulfur clusters within the iron-sulfur subunit requires further analysis, such as electron paramagnetic resonance. One possible explanation for the absence of Fe-S clusters in the iron-sulfur subunit could be the compatibility issue between the Fe-S cluster synthesis machinery and the expressed iron-sulfur subunits. Three major Fe-S cluster synthesis machineries have been reported which are called the NIF machinery, ISC machinery, and SUF machinery, respectively[78] (Fig. 2.9). Several Fe-S cluster synthesis machineries are present in *E. coli*: ISC[79], SUF[80], and CsdAE[81]. ISC is the main machinery for Fe-S cluster synthesis[79], SUF is utilized under conditions of iron starvation and oxidative stress[80]. For the iron-sulfur subunit of SDH, ISC, and HscAE, Fe-S cluster biosynthetic chaperones, are important for Fe-S cluster insertion, especially [2Fe-2S][82]. In contrast, *B. subtilis* contains a slightly different SUF-type machinery, called Bacilli-SUF, and the SDH iron-sulfur subunit

is matured by SufU-related mechanisms[83]. Among the Gram-positive bacteria, Clostridia-ISC, Actinobacteria-SUF, and Bacilli-SUF have been reported[84]. *C. glutamicum* contains the Bacilli-SUF-type machinery, and the *P. thermopropionicum* genome contains the Clostridia-ISC-type machinery. The protein sequences of the iron-sulfur subunits of *C. glutamicum* and *B. subtilis* are phylogenetically closely related, but the homology was not high (AA identity: 26.7%), The reason why the iron-sulfur subunits of *B. subtilis* and *P. thermopropionicum* lack Fe-S clusters in *E. coli* remain unclear; however, a specific Fe-S cluster synthesis machinery is probably required for heterologously expressed SDH to function.

Finally, based on the information we found about flavinylation and Fe-S clusters, solving these problems and enabling the comparison and high expression levels of SDH from Gram-positive bacteria, which has not been attempted in *E. coli*, may be possible. In other words, analyzing and comparing SDHs in cells derived from microorganisms that have not yet been cultured or from parasitic pathogenic bacteria may be easier. Further studies are required to obtain the activity levels of SDH from *B. subtilis* and *P. thermopropionicum* in *E. coli*.

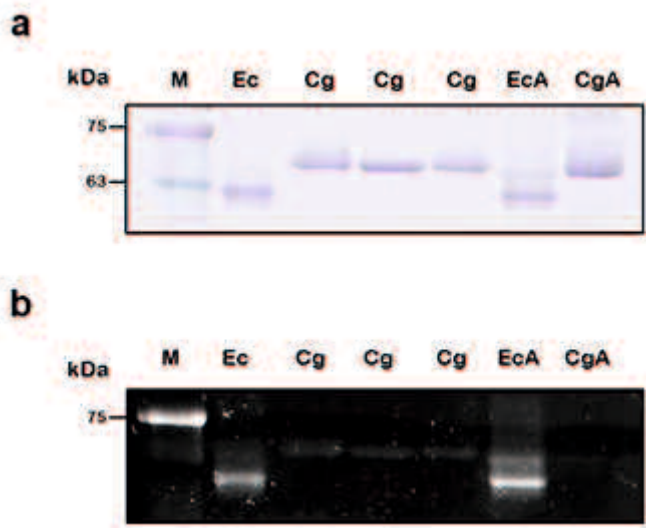

Fig. 2.8 Comparison of in-gel fluorescence of covalently bound FAD to the same gel in *E. coli* and *C. glutamicum*.

The purified SDH flavoprotein subunits used are the same as in Fig. 1 and the purified SDH complex is the same as in Fig. 2. UV irradiation was used to detect of the fluorescence of covalently bound FAD. The purified *C. glutamicum* SDH complex used three independently samples. (a) CBB-stained. Each sample loaded 1 μg. (b) In-gel fluorescence of covalently bound FAD in flavoproteins with acetic acid treatment. M: molecular marker; Ec: *E. coli* SDH complex; Cg: *C. glutamicum* SDH complex; EcA: *E. coli* SDH flavoprotein subunit; CgA: *C. glutamicum* SDH flavoprotein subunit.

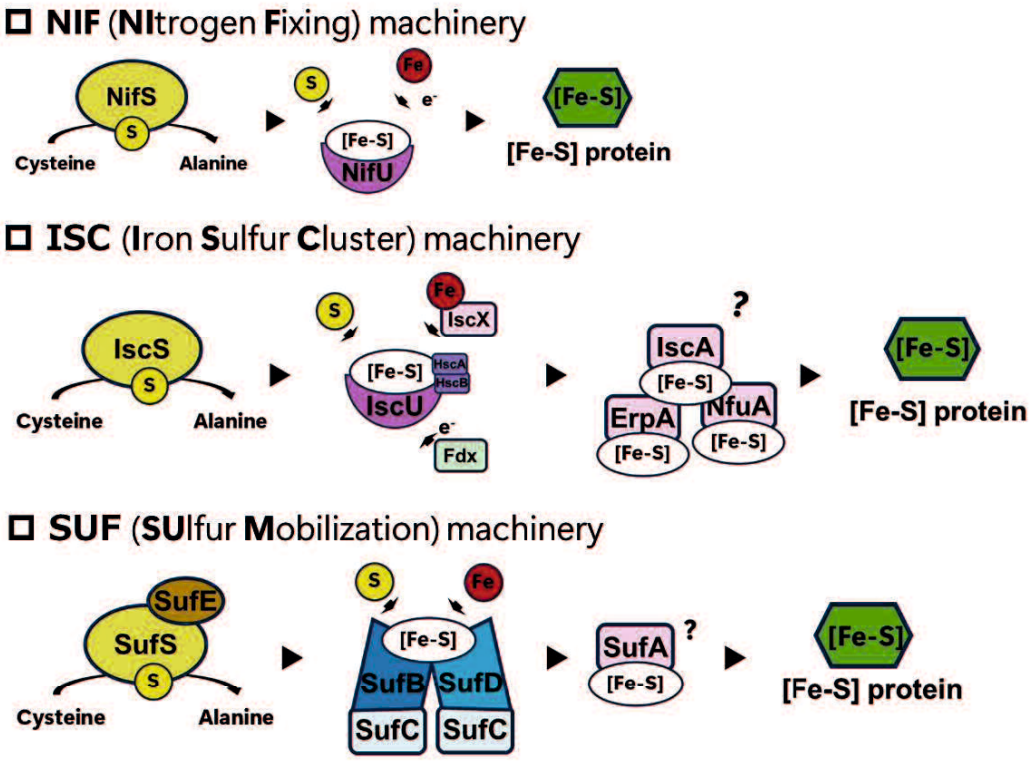

Fig. 2.9 Models of Three Major Fe-S Cluster Biosynthesis Machineries

In these systems, a cysteine desulfurase (NifS / IscS / SufS) extracts a sulfur atom from L-cysteine, which serves as the sulfur source. Subsequently, novel Fe-S clusters are assembled on scaffold proteins (NifU / IscU / SufBCD).

2.5 CONCLUSION

Flavinylation of the flavoprotein subunit of Type B SDH from Gram-positive bacteria did not occur when it was heterologously expressed in *E. coli*. However, when the iron-sulfur cluster and the membrane subunits were co-expressed, covalent binding of FAD was observed. This finding was confirmed in vitro, suggesting that the covalent binding of FAD to the flavoprotein of Type B SDH from Gram-positive bacteria was assisted by the presence of fumarate or an iron-sulfur subunit. Conversely, in functionally heterologously expressed SDH, the maturation of the iron-sulfur cluster emerges as an important process, along with the need for FAD binding to the flavoprotein subunit.

2.6 PUBLICATION

This chapter represents an expanded version of the work originally published in: Yusuke Shiota and Tomoyuki Kosaka, "Insight on flavinylation and functioning factor in Type B succinate dehydrogenase from Gram-positive bacteria" Bioscience, Biotechnology, and Biochemistry, 2025 89 832-840.

DOI: https://doi.org/10.1093/bbb/zbaf026

ADDITIONAL DISCUSSION

Throughout Chapter 1 and Chapter 2 demonstrated the functional and genetic features of *P. thermopropionicum* SDH and showed that SDHs from Gram-positive bacteria share a common FAD-binding mechanism but involve a species-specific machinery for the synthesis of iron-sulfur clusters, respectively. This is due to differences in the environment in which microorganisms live and each subunit of SDH may employ a species-specific optimized maturation mechanism.

Heterologous expression of SDH from *E. coli*, *C. glutamicum*, and *P. thermopropionicum* was performed using *B. subtilis* as a host. All heterologously expressed SDH strains were observed no succinate oxidizing and fumarate reducing activities (Fig. 3.1). Gram-positive bacteria have a variety of specific iron-sulfur cluster synthesis mechanisms and employ a species-specific iron-sulfur cluster synthesis machinery[84]. These results support the need to employ the appropriate iron-sulfur cluster synthesis machinery for each SDH for the functional heterologous expression of SDHs showed in Chapter 2. Surprisingly, *E. coli* and *P. thermopropionicum* SDH and *E. coli* FRD were heterologously expressed in *C. glutamicum* as host, *E. coli* SDH observed a slight succinate oxidizing activity and *E. coli* FRD observed fumarate reducing activity. (Fig. 3.2). It has been suggested that the flavinylation of the *E. coli* SDH flavoprotein subunit occurs when the caller concentration of fumarate in the cell increases even in the absence of FAD-binding protein and it may be enhanced in under anaerobic and microaerophilic conditions or roughly 20°C or higher. This hypothesis supported by *In vitro* demonstration shown that flavinylation of *E. coli* SDH flavoprotein subunit occurs in the presence of 20 mM fumarate in the absence of *sdhE*[17] and also by my previous shown that SDH activity was observed in an *E. coli* Δ*sdh*Δ*frd*Δ*sdhE* strain SDH complemented by plasmid cultured at 30°C and flavinylation occurred when the flavoprotein subunit was expressed (Date not shown). However, it is unclear why the SDH maturation mechanism of *E. coli* and *C. glutamicum* that employ completely different iron-sulfur cluster synthesis machinery can complement each other, whereas the maturation of *B. subtilis* and *C. glutamicum* that employ the same type of iron-sulfur cluster synthesis machinery cannot complement each other. Further genetic and biochemical analyses are required to clarify this problem.

Our study demonstrated that the FAD-binding motifs and alignment of membrane-bound subunits SDH of *P. thermopropionicum* possess specific conserved amino acid residues that are strongly associated with efficient succinate oxidation in syntrophic propionate-oxidizing bacteria, and heterologously expressed SDH suggested of *P. thermopropionicum* that the covalent FAD binding mechanism is common to *B. subtilis* and *C. glutamicum*. The iron-sulfur cluster synthesis machinery also able to predict from the *P. thermopropionicum* genome. Further research is required to the SDH of *P. thermopropionicum* functioning in heterologous expression cells, such as co-expression the iron-sulfur cluster synthesis mechanism of *P. thermopropionicum*. However, the use of heterologously

expressed technology is expected to clarify whether a membrane potential is required for succinate oxidation even in thermophilic propionate-oxidizing bacteria and to gain further insights.

This finding from this study suggests that even enzymes conserved across many wide range species have species-specific optimized utilization strategies. These strategies can be demonstrated under heterologous cells and *in vitro* condition using heterologously expressed technology, even for species that the genetic recombination technology has not been established and the culture is complicated. These findings will help us isolation culture and utilize unique microorganisms that are currently uncultivable.

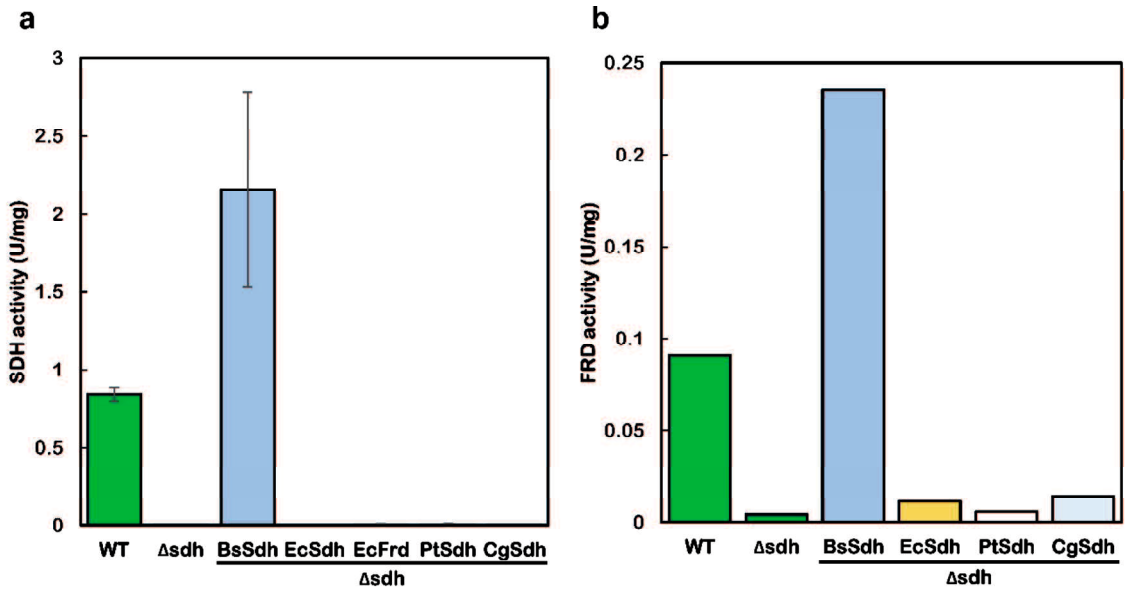

Fig. 3.1 Enzyme activity of cell Extract prepared from *B. subtilis* Δsdh harboring heterologously expressed SDHs

Strains were cultured in 150 ml of LB medium containing 50 mM MOPS and 20 μM chloramphenicol on 30°C at 200rpm 20h. Various SDHs were heterologously expressed in a pHCMC02-based vector by B. subtilis sdhC promoter. a, SDH activity was determined by DCIP as electron acceptor. PMS reduction was determined by monitoring the absorbance at 600 nm at room temperature in a solution containing 16.6 mM phosphate buffer, 0.2 mM PMS, 0.11 mM DCIP, 20 mM succinate and each sample. The reaction was initiated by the addition of succinate. b, FRD activity was determined by Benzyl viologen (BV) as electron donor. BV reduction was determined by monitoring the absorbance at 550 nm at room temperature in a solution containing 50 mM phosphate buffer, 0.1 mM BV, 20 mM fumarate. BV was reduced with dithionite before adding the samples. The reaction was initiated by the addition of fumarate. WT; *B. subtilis* 168; Δsdh; *B. subtilis* sdh operon deletion strain; BsSdh: *B. subtilis* SDH; EcSdh: *E. coli* SDH; EcFdh: *E. coli* fumarate reductase (FRD); CgSdh: *C. glutamicum* SDH; PtSdh: *P. thermopropionicum* SDH.

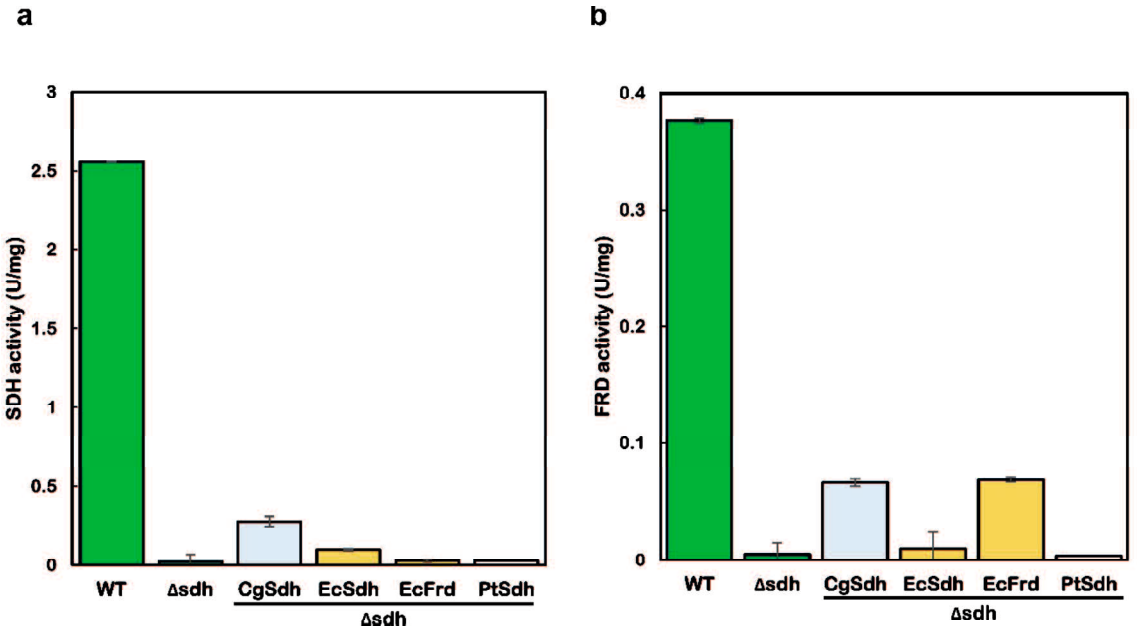

Fig. 3.2 Enzyme activity of cell Extract prepared from *C. glutamicum* Δsdh harboring heterologously expressed SDHs

Strains were cultured in 150 ml of P7 medium containing 50 μg/mL kanamycin and 0.1 mM IPTG on 30°C at 200rpm 20h. Various SDHs were heterologously expressed in a pCNKS-based vector by B. subtilis sdhC promoter. a, SDH activity was determined by DCIP as electron acceptor. PMS reduction was determined by monitoring the absorbance at 600 nm at room temperature in a solution containing 16.6 mM phosphate buffer, 0.2 mM PMS, 0.11 mM DCIP, 20 mM succinate and each sample. The reaction was initiated by the addition of succinate. b, FRD activity was determined by BV as electron donor. BV reduction was determined by monitoring the absorbance at 550 nm at room temperature in a solution containing 50 mM phosphate buffer, 0.1 mM BV, 20 mM fumarate. BV was reduced with dithionite before adding the samples. The reaction was initiated by the addition of fumarate. WT; *C. glutamicum* ATCC13032; Δsdh; *C. glutamicum* sdh operon deletion strain; CgSdh: *C. glutamicum* SDH; EcSdh: *E. coli* SDH; EcFdh: *E. coli* FRD; PtSdh: *P. thermopropionicum* SDH.

REFERENCE

1. Tanoue, T., Morita, S., Plichta, D.R., Skelly, A.N., Suda, W., Sugiura, Y., Narushima, S., Vlamakis, H., Motoo, I., and Sugita, K. (2019). A defined commensal consortium elicits CD8 T cells and anti-cancer immunity. Nature *565*, 600-605.
2. Merino, N., Aronson, H.S., Bojanova, D.P., Feyhl-Buska, J., Wong, M.L., Zhang, S., and Giovannelli, D. (2019). Living at the extremes: extremophiles and the limits of life in a planetary context. Frontiers in microbiology *10*, 780.
3. 小柳喬 (2021). 伝統発酵食品における微生物発酵様式の多様性・頑健性と細菌叢形成の特徴. 日本食品微生物学会雑誌 *38*, 1-8.
4. 高岡大造 (2021). 微生物燃料電池. 実験力学 *21*, 57-59.
5. Yoshida, S., Hiraga, K., Takehana, T., Taniguchi, I., Yamaji, H., Maeda, Y., Toyohara, K., Miyamoto, K., Kimura, Y., and Oda, K. (2016). A bacterium that degrades and assimilates poly (ethylene terephthalate). Science *351*, 1196-1199.
6. Hägerhäll, C. (1997). Succinate: quinone oxidoreductases: variations on a conserved theme. Biochimica et Biophysica Acta (BBA)-Bioenergetics *1320*, 107-141.
7. Lancaster, C.R.D. (2002). Succinate: quinone oxidoreductases: an overview. Biochimica et Biophysica Acta (BBA)-Bioenergetics *1553*, 1-6.
8. Cecchini, G. (2003). Function and structure of complex II of the respiratory chain. Annual review of biochemistry *72*, 77-109.
9. Owen, O.E., Kalhan, S.C., and Hanson, R.W. (2002). The key role of anaplerosis and cataplerosis for citric acid cycle function. Journal of Biological Chemistry *277*, 30409-30412.
10. Kosaka, T., Uchiyama, T., Ishii, S.-i., Enoki, M., Imachi, H., Kamagata, Y., Ohashi, A., Harada, H., Ikenaga, H., and Watanabe, K. (2006). Reconstruction and regulation of the central catabolic pathway in the thermophilic propionate-oxidizing syntroph *Pelotomaculum thermopropionicum*. Journal of bacteriology *188*, 202-210.
11. Stams, A.J., and Plugge, C.M. (2009). Electron transfer in syntrophic communities of anaerobic bacteria and archaea. Nature Reviews Microbiology *7*, 568-577.
12. Mei, R., Nobu, M.K., and Liu, W.T. (2020). Identifying anaerobic amino acids degraders through the comparison of short-term and long-term enrichments. Environmental Microbiology Reports *12*, 173-184.
13. Imachi, H., Sekiguchi, Y., Kamagata, Y., Hanada, S., Ohashi, A., and Harada, H. (2002). *Pelotomaculum thermopropionicum* gen. nov., sp. nov., an anaerobic, thermophilic, syntrophic propionate-oxidizing bacterium. International journal of systematic and evolutionary microbiology *52*, 1729-1735.
14. Kato, S., Kosaka, T., and Watanabe, K. (2009). Substrate-dependent transcriptomic shifts in *Pelotomaculum thermopropionicum* grown in syntrophic co-culture with *Methanothermobacter thermautotrophicus*. Microbial biotechnology *2*, 575-584.

15. Schink, B. (1997). Energetics of syntrophic cooperation in methanogenic degradation. Microbiology and molecular biology reviews *61*, 262-280.
16. Kounosu, A. (2014). Analysis of covalent flavinylation using thermostable succinate dehydrogenase from *Thermus thermophilus* and *Sulfolobus tokodaii* lacking SdhE homologs. FEBS letters *588*, 1058-1063.
17. Maklashina, E., Iverson, T.M., and Cecchini, G. (2022). How an assembly factor enhances covalent FAD attachment to the flavoprotein subunit of complex II. Journal of Biological Chemistry *298*, 102472.
18. Kosaka, T., Tsushima, Y., Shiota, Y., Ishiguchi, T., Matsushita, K., Matsutani, M., and Yamada, M. (2023). Membrane Potential-requiring Succinate Dehydrogenase Constitutes the Key to Propionate Oxidation and Is Unique to Syntrophic Propionate-oxidizing Bacteria. Microbes and environments *38*, ME22111.
19. Leng, L., Yang, P., Singh, S., Zhuang, H., Xu, L., Chen, W.-H., Dolfing, J., Li, D., Zhang, Y., and Zeng, H. (2018). A review on the bioenergetics of anaerobic microbial metabolism close to the thermodynamic limits and its implications for digestion applications. Bioresource technology *247*, 1095-1106.
20. Jackson, B.E., and McInerney, M.J. (2002). Anaerobic microbial metabolism can proceed close to thermodynamic limits. Nature *415*, 454-456.
21. Houwen, F.P., Plokker, J., Stams, A.J., and Zehnder, A.J. (1990). Enzymatic evidence for involvement of the methylmalonyl-CoA pathway in propionate oxidation by *Syntrophobacter wolinii*. Archives of microbiology *155*, 52-55.
22. de Bok, F.A., Stams, A.J., Dijkema, C., and Boone, D.R. (2001). Pathway of propionate oxidation by a syntrophic culture of Smithella propionica and *Methanospirillum hungatei*. Applied and environmental microbiology *67*, 1800-1804.
23. Dyksma, S., and Gallert, C. (2019). Candidatus *Syntrophosphaera thermopropionivorans*: a novel player in syntrophic propionate oxidation during anaerobic digestion. Environmental microbiology reports *11*, 558-570.
24. Müller, N., Worm, P., Schink, B., Stams, A.J., and Plugge, C.M. (2010). Syntrophic butyrate and propionate oxidation processes: from genomes to reaction mechanisms. Environmental microbiology reports *2*, 489-499.
25. Imachi, H., Sekiguchi, Y., Kamagata, Y., Ohashi, A., and Harada, H. (2000). Cultivation and in situ detection of a thermophilic bacterium capable of oxidizing propionate in syntrophic association with hydrogenotrophic methanogens in a thermophilic methanogenic granular sludge. Applied and Environmental Microbiology *66*, 3608-3615.
26. Kosaka, T., Kato, S., Shimoyama, T., Ishii, S., Abe, T., and Watanabe, K. (2008). The genome of *Pelotomaculum thermopropionicum* reveals niche-associated evolution in anaerobic microbiota. Genome research *18*, 442-448.
27. Kosaka, T., Toh, H., Fujiyama, A., Sakaki, Y., Watanabe, K., Meng, X.Y., Hanada, S., and Toyoda, A. (2014). Physiological and genetic basis for self-aggregation of a thermophilic hydrogenotrophic methanogen, *Methanothermobacter* strain CaT 2. Environmental Microbiology Reports *6*, 268-277.

28. Matsushita, K., YAMADA, M., SHINAGAWA, E., ADACHI, O., and AMEYAMA, M. (1980). Function of ubiquinone in the electron transport system of Pseudomonas aeruginosa grown aerobically. The Journal of Biochemistry *88*, 757-764.

29. Redfearn, E. (1967). [68] Isolation and determination of ubiquinone. In Methods in enzymology, (Elsevier), pp. 381-384.

30. Matsushita, K., Ohnishi, T., and Kaback, H.R. (1987). NADH-ubiquinone oxidoreductases of the *Escherichia coli* aerobic respiratory chain. Biochemistry *26*, 7732-7737.

31. Altschul, S.F., Madden, T.L., Schäffer, A.A., Zhang, J., Zhang, Z., Miller, W., and Lipman, D.J. (1997). Gapped BLAST and PSI-BLAST: a new generation of protein database search programs. Nucleic acids research *25*, 3389-3402.

32. Edgar, R.C. (2004). MUSCLE: multiple sequence alignment with high accuracy and high throughput. Nucleic acids research *32*, 1792-1797.

33. Edgar, R.C. (2004). MUSCLE: a multiple sequence alignment method with reduced time and space complexity. BMC bioinformatics *5*, 1-19.

34. Tamura, K., Dudley, J., Nei, M., and Kumar, S. (2007). MEGA4: molecular evolutionary genetics analysis (MEGA) software version 4.0. Molecular biology and evolution *24*, 1596-1599.

35. Stecher, G., Tamura, K., and Kumar, S. (2020). Molecular evolutionary genetics analysis (MEGA) for macOS. Molecular biology and evolution *37*, 1237-1239.

36. Van Dongen, S., and Abreu-Goodger, C. (2011). Using MCL to extract clusters from networks. In Bacterial molecular networks: Methods and protocols, (Springer), pp. 281-295.

37. Wallrabenstein, C., and Schink, B. (1994). Evidence of reversed electron transport in syntrophic butyrate or benzoate oxidation by *Syntrophomonas wolfei* and *Syntrophus buswellii*. Archives of microbiology *162*, 136-142.

38. Grivennikova, V.G., and Vinogradov, A.D. (1982). Kinetics of ubiquinone reduction by the resolved succinate: ubiquinone reductase. Biochimica et Biophysica Acta (BBA)-Bioenergetics *682*, 491-495.

39. Horsefield, R., Yankovskaya, V., Sexton, G., Whittingham, W., Shiomi, K., Ōmura, S., Byrne, B., Cecchini, G., and Iwata, S. (2006). Structural and computational analysis of the quinone-binding site of complex II (succinate-ubiquinone oxidoreductase): a mechanism of electron transfer and proton conduction during ubiquinone reduction. Journal of Biological Chemistry *281*, 7309-7316.

40. Lancaster, C.R.D. (2013). The di-heme family of respiratory complex II enzymes. Biochimica et Biophysica Acta (BBA)-Bioenergetics *1827*, 679-687.

41. Cheng, V.W., Piragasam, R.S., Rothery, R.A., Maklashina, E., Cecchini, G., and Weiner, J.H. (2015). Redox state of flavin adenine dinucleotide drives substrate binding and product release in *Escherichia coli* succinate dehydrogenase. Biochemistry *54*, 1043-1052.

42. Guan, H.-H., Hsieh, Y.-C., Lin, P.-J., Huang, Y.-C., Yoshimura, M., Chen, L.-Y., Chen, S.-K., Chuankhayan, P., Lin, C.-C., and Chen, N.-C. (2018). Structural insights into the electron/proton transfer pathways in the

quinol: fumarate reductase from *Desulfovibrio gigas*. Scientific Reports *8*, 14935.

43. Maklashina, E., Iverson, T.M., Sher, Y., Kotlyar, V., Andréll, J., Mirza, O., Hudson, J.M., Armstrong, F.A., Rothery, R.A., and Weiner, J.H. (2006). Fumarate reductase and succinate oxidase activity of *Escherichia coli* complex II homologs are perturbed differently by mutation of the flavin binding domain. Journal of biological chemistry *281*, 11357-11365.

44. Lancaster, C.R.D., Sauer, U.S., Groß, R., Haas, A.H., Graf, J., Schwalbe, H., Mäntele, W., Simon, J., and Madej, M.G. (2005). Experimental support for the "E pathway hypothesis" of coupled transmembrane e– and H+ transfer in dihemic quinol: fumarate reductase. Proceedings of the National Academy of Sciences *102*, 18860-18865.

45. Hidalgo-Ahumada, C.A., Nobu, M.K., Narihiro, T., Tamaki, H., Liu, W.T., Kamagata, Y., Stams, A.J., Imachi, H., and Sousa, D.Z. (2018). Novel energy conservation strategies and behaviour of *Pelotomaculum schinkii* driving syntrophic propionate catabolism. Environmental Microbiology *20*, 4503-4511.

46. Pinske, C., Jaroschinsky, M., Linek, S., Kelly, C.L., Sargent, F., and Sawers, R.G. (2015). Physiology and bioenergetics of [NiFe]-hydrogenase 2-catalyzed H2-consuming and H2-producing reactions in *Escherichia coli*. Journal of bacteriology *197*, 296-306.

47. Schirawski, J., and Unden, G. (1998). Menaquinone-dependent succinate dehydrogenase of bacteria catalyzes reversed electron transport driven by the proton potential. European journal of biochemistry *257*, 210-215.

48. Zaunmuller, T., Kelly, D.J., Glockner, F.O., and Unden, G. (2006). Succinate dehydrogenase functioning by a reverse redox loop mechanism and fumarate reductase in sulphate-reducing bacteria. Microbiology *152*, 2443-2453.

49. Madej, M.G., Nasiri, H.R., Hilgendorff, N.S., Schwalbe, H., Unden, G., and Lancaster, C.R.D. (2006). Experimental evidence for proton motive force-dependent catalysis by the diheme-containing succinate: menaquinone oxidoreductase from the Gram-positive bacterium *Bacillus licheniformis*. Biochemistry *45*, 15049-15055.

50. Lancaster, C.R.D., Haas, A.H., Madej, M.G., and Mileni, M. (2006). Recent progress on obtaining theoretical and experimental support for the "E-pathway hypothesis" of coupled transmembrane electron and proton transfer in dihaem-containing quinol: fumarate reductase. Biochimica et Biophysica Acta (BBA)-Bioenergetics *1757*, 988-995.

51. Madej, M.G., Müller, F.G., Ploch, J., and Lancaster, C.R.D. (2009). Limited reversibility of transmembrane proton transfer assisting transmembrane electron transfer in a dihaem-containing succinate: quinone oxidoreductase. Biochimica et Biophysica Acta (BBA)-Bioenergetics *1787*, 593-600.

52. Gabaldón, T., Rainey, D., and Huynen, M.A. (2005). Tracing the evolution of a large protein complex in the eukaryotes, NADH: ubiquinone oxidoreductase (Complex I). Journal of molecular biology *348*, 857-870.

53. Salach, J., Walker, W.H., Singer, T.P., Ehrenberg, A., Hemmerich, P., Ghisla, S., and Hartmann, U. (1972). Studies on Succinate Dehydrogenase: Site of Attachment of the Covalently-Bound Flavin to the Peptide

Chain. European Journal of Biochemistry *26*, 267-278.

54. Cheng, V.W., Ma, E., Zhao, Z., Rothery, R.A., and Weiner, J.H. (2006). The iron-sulfur clusters in *Escherichia coli* succinate dehydrogenase direct electron flow. Journal of Biological Chemistry *281*, 27662-27668.

55. Hards, K., Rodriguez, S.M., Cairns, C., and Cook, G.M. (2019). Alternate quinone coupling in a new class of succinate dehydrogenase may potentiate mycobacterial respiratory control. FEBS letters *593*, 475-486.

56. Nakamura, K., Yamaki, M., Sarada, M., Nakayama, S., Vibat, C.R.T., Gennis, R.B., Nakayashiki, T., Inokuchi, H., Kojima, S., and Kita, K. (1996). Two Hydrophobic Subunits Are Essential for the Heme b Ligation and Functional Assembly of Complex II (Succinate-Ubiquinone Oxidoreductase) from *Escherichia coli* (∗). Journal of Biological Chemistry *271*, 521-527.

57. Maher, M.J., Herath, A.S., Udagedara, S.R., Dougan, D.A., and Truscott, K.N. (2018). Crystal structure of bacterial succinate: quinone oxidoreductase flavoprotein SdhA in complex with its assembly factor SdhE. Proceedings of the National Academy of Sciences *115*, 2982-2987.

58. Heuts, D.P., Scrutton, N.S., McIntire, W.S., and Fraaije, M.W. (2009). What's in a covalent bond? On the role and formation of covalently bound flavin cofactors. The FEBS journal *276*, 3405-3427.

59. Hao, H.-X., Khalimonchuk, O., Schraders, M., Dephoure, N., Bayley, J.-P., Kunst, H., Devilee, P., Cremers, C.W., Schiffman, J.D., and Bentz, B.G. (2009). SDH5, a gene required for flavination of succinate dehydrogenase, is mutated in paraganglioma. Science *325*, 1139-1142.

60. McNeil, M.B., Clulow, J.S., Wilf, N.M., Salmond, G.P., and Fineran, P.C. (2012). SdhE is a conserved protein required for flavinylation of succinate dehydrogenase in bacteria. Journal of Biological Chemistry *287*, 18418-18428.

61. Sharma, P., Maklashina, E., Cecchini, G., and Iverson, T. (2020). The roles of SDHAF2 and dicarboxylate in covalent flavinylation of SDHA, the human complex II flavoprotein. Proceedings of the National Academy of Sciences *117*, 23548-23556.

62. Hederstedt, L., Bergman, T., and Jörnvall, H. (1987). Processing of *Bacillus subtilis* succinate dehydrogenase and cytochrome &-558 polypeptides: Lack of covalently bound flavin in the Bacillus enzyme expressed in Escherichia coli. FEBS letters *213*, 385-390.

63. Ruprecht, J., Yankovskaya, V., Maklashina, E., Iwata, S., and Cecchini, G. (2009). Structure of *Escherichia coli* succinate: quinone oxidoreductase with an occupied and empty quinone-binding site. Journal of Biological Chemistry *284*, 29836-29846.

64. Sheneman, L., Evans, J., and Foster, J.A. (2006). Clearcut: a fast implementation of relaxed neighbor joining. Bioinformatics *22*, 2823-2824.

65. Datsenko, K.A., and Wanner, B.L. (2000). One-step inactivation of chromosomal genes in *Escherichia coli* K-12 using PCR products. Proceedings of the National Academy of Sciences *97*, 6640-6645.

66. Gibson, D.G., Young, L., Chuang, R.-Y., Venter, J.C., Hutchison III, C.A., and Smith, H.O. (2009). Enzymatic assembly of DNA molecules up to several hundred kilobases. Nature methods *6*, 343-345.

67. Nakayama, H., and Shimamoto, N. (2014). Modern and simple construction of plasmid: saving time and cost. Journal of Microbiology *52*, 891-897.

68. Kiefler, I., Bringer, S., and Bott, M. (2015). SdhE-dependent formation of a functional *Acetobacter pasteurianus* succinate dehydrogenase in *Gluconobacter oxydans*—a first step toward a complete tricarboxylic acid cycle. Applied microbiology and biotechnology *99*, 9147-9160.

69. Cecchini, G., Schröder, I., Gunsalus, R.P., and Maklashina, E. (2002). Succinate dehydrogenase and fumarate reductase from *Escherichia coli*. Biochimica et Biophysica Acta (BBA)-Bioenergetics *1553*, 140-157.

70. Kurokawa, T., and Sakamoto, J. (2005). Purification and characterization of succinate: menaquinone oxidoreductase from *Corynebacterium glutamicum*. Archives of microbiology *183*, 317-324.

71. Hederstedt, L., and Andersson, K.K. (1986). Electron-paramagnetic-resonance spectroscopy of *Bacillus subtilis* cytochrome b_{558} in *Escherichia coli* membranes and in succinate dehydrogenase complex from *Bacillus subtilis* membranes. Journal of bacteriology *167*, 735-739.

72. Wang, P.-H., Nishikawa, S., McGlynn, S.E., and Fujishima, K. (2023). One-pot de novo synthesis of [4Fe-4S] proteins using a recombinant SUF system under aerobic conditions. ACS Synthetic Biology *12*, 2887-2896.

73. Kim, J., Fuller, J.H., Kuusk, V., Cunane, L., Chen, Z.-w., Mathews, F.S., and McIntire, W.S. (1995). The Cytochrome Subunit Is Necessary for Covalent FAD Attachment to the Flavoprotein Subunit of p-Cresol Methylhydroxylase (∗). Journal of Biological Chemistry *270*, 31202-31209.

74. Cunane, L.M., Chen, Z.-w., McIntire, W.S., and Mathews, F.S. (2005). p-Cresol methylhydroxylase: alteration of the structure of the flavoprotein subunit upon its binding to the cytochrome subunit. Biochemistry *44*, 2963-2973.

75. Scrutton, N.S., Packman, L.C., Mathews, F.S., Rohlfs, R.J., and Hille, R. (1994). Assembly of redox centers in the trimethylamine dehydrogenase of bacterium W3A1. Properties of the wild-type enzyme and a C30A mutant expressed from a cloned gene in *Escherichia coli*. Journal of Biological Chemistry *269*, 13942-13950.

76. Kim, H.J., Jeong, M.-Y., Na, U., and Winge, D.R. (2012). Flavinylation and assembly of succinate dehydrogenase are dependent on the C-terminal tail of the flavoprotein subunit. Journal of Biological Chemistry *287*, 40670-40679.

77. Hederstedt, L. (1983). Succinate Dhydrogenase Mutants of Bacillus Suybtilis Lacking Covalently Bound Flavin in the Flavoprotien Subunit. European Journal of Biochemistry *132*, 589-593.

78. Hidese, R., Mihara, H., and Esaki, N. (2011). Bacterial cysteine desulfurases: versatile key players in biosynthetic pathways of sulfur-containing biofactors. Applied microbiology and biotechnology *91*, 47-61.

79. Schwartz, C.J., Djaman, O., Imlay, J.A., and Kiley, P.J. (2000). The cysteine desulfurase, IscS, has a major role in in vivo Fe-S cluster formation in *Escherichia coli*. Proceedings of the National Academy of Sciences *97*, 9009-9014.

80. Outten, F.W., Djaman, O., and Storz, G. (2004). A suf operon requirement for Fe–S cluster assembly during iron starvation in *Escherichia coli*. Molecular microbiology *52*, 861-872.

81. Loiseau, L., Ollagnier-de Choudens, S., Lascoux, D., Forest, E., Fontecave, M., and Barras, F. (2005). Analysis of the heteromeric CsdA-CsdE cysteine desulfurase, assisting Fe-S cluster biogenesis in *Escherichia coli*. Journal of Biological Chemistry *280*, 26760-26769.

82. Tokumoto, U., and Takahashi, Y. (2001). Genetic analysis of the isc operon in *Escherichia coli* involved in the biogenesis of cellular iron-sulfur proteins. The Journal of biochemistry *130*, 63-71.

83. Albrecht, A.G., Netz, D.J., Miethke, M., Pierik, A.J., Burghaus, O., Peuckert, F., Lill, R., and Marahiel, M.A. (2010). SufU is an essential iron-sulfur cluster scaffold protein in *Bacillus subtilis*. Journal of bacteriology *192*, 1643-1651.

84. Dos Santos, P.C. (2014). Fe-S assembly in Gram-positive bacteria. Iron sulfur clusters in chemistry and biology *1*.

ACKNOWLEDGMENTS

First of all, I would like to express my sincere gratitude to my advisor Pref. Dr. Tomoyuki Kosaka for their continuous support of my study and research since my undergraduate days, for their patience, motivation, enthusiasm, and immense knowledge. Their guidance helped me throughout the research and writing of this thesis. I could not have imagined having a better advisor and mentor for my Ph.D. studies.

This Ph.D. research was supported by JST SPRING (Grant No. JPMJSP2111). *B. subtilis* and vector plasmid were kindly provided by Prof. Dr. Hirofumi Yoshikawa and Prof. Dr. Kei Asai of Tokyo University of Agriculture. *C. glutamicum* and vector plasmid were kindly provided by Asso. Pref. Dr. Naoya Kataoka of Yamaguchi University. I would like to express my sincere gratitude.

Besides my advisor, I would like to thank Prof. Dr. Toshiharu Yakushi, Asso. Pref. Dr. Naoya Kataoka, Prof. Dr. Kazunobu Matsushita and Prof. Dr. Mamoru Yamada for their helpful discussions. I would also like to thank Dr. Minenosuke Matsutani for collaboration research.

I express our sincere thanks to Yuka Tsushima, Takayuki Ishiguchi, and Kazuo Matsushita for collaboration study and thanks are extended to the members of Information Biochemistry Laboratory and Laboratory for functions of microorganisms for their every support.

Finally, my deepest gratitude goes to my family for their unflagging love and support for not only my Ph.D. research but also for throughout my life; this dissertation is simply impossible without them.